The Institute of OPTICS

PRAISE
Phase Retrieval & Imaging Science

Phase Retrieval and Support Estimation in X-Ray Diffraction

James R. Fienup

Robert E. Hopkins Professor of Optics

University of Rochester
Institute of Optics

Presented to Coherence 2005: International Workshop on Phase Retrieval and Coherent Scattering (DESY-ESRF-SLS)
15 June, 2005

IGeSA, Island of Porquerolles, France

Outline

- Phase retrieval applications

- Phase retrieval algorithms
  - Iterative Transform Algorithm
    - Hybrid input-output algorithm
  - Gradient search algorithms

- Support Constraint
  - Importance
  - Reconstructing object support from autocorrelation support
  - Tightening the support constraint
  - Several examples

Phase Retrieval Application: Imaging through Atmospheric Turbulence

- Problem: atmospheric turbulence causes phase errors, limits resolution

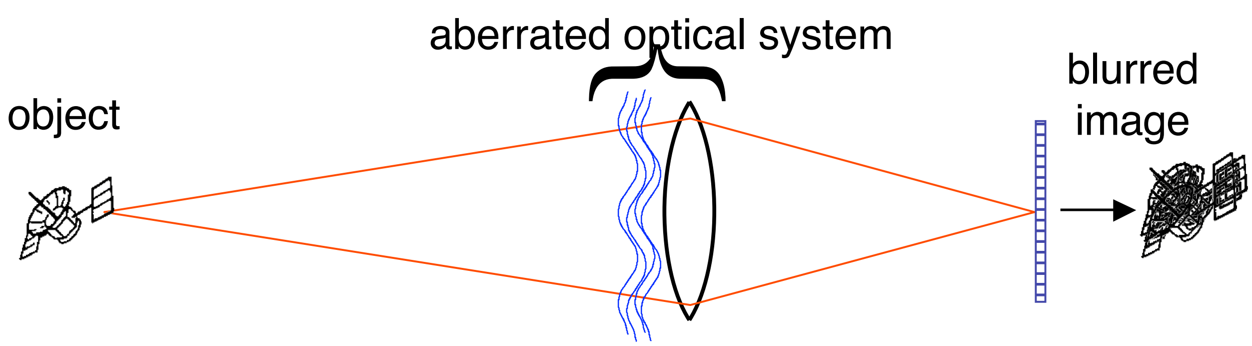

- Labeyrie's stellar speckle interferometry yields Fourier magnitude
  - Incoherent (real, nonnegative) image
- Lensless imaging with laser illumination
  - Measure far-field speckle intensity
  - Complex-valued image
- Both mathematically similar to x-ray diffraction

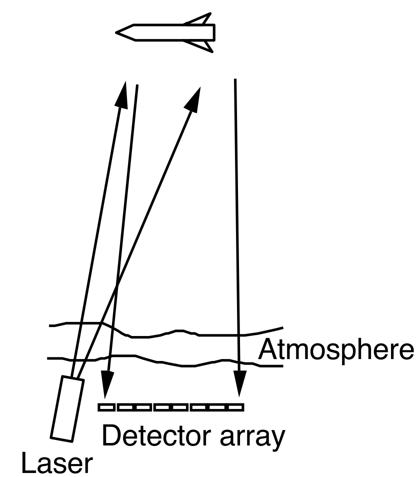

PROCLAIM 3-D Imaging Concept

Phase Retrieval with Opacity Constraint LAser IMaging

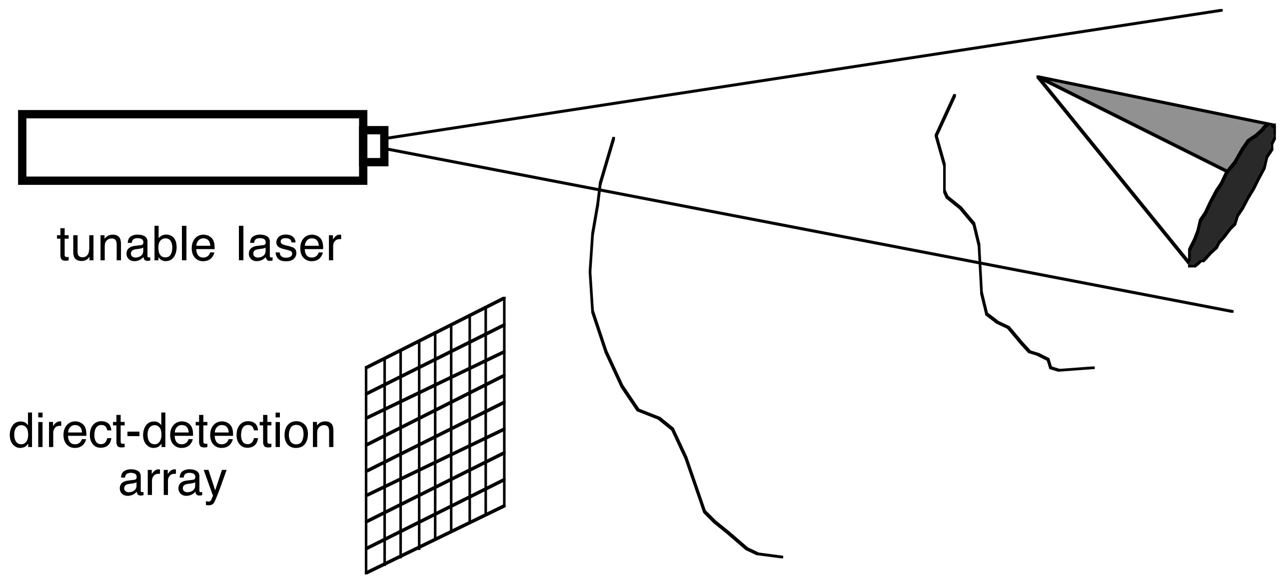

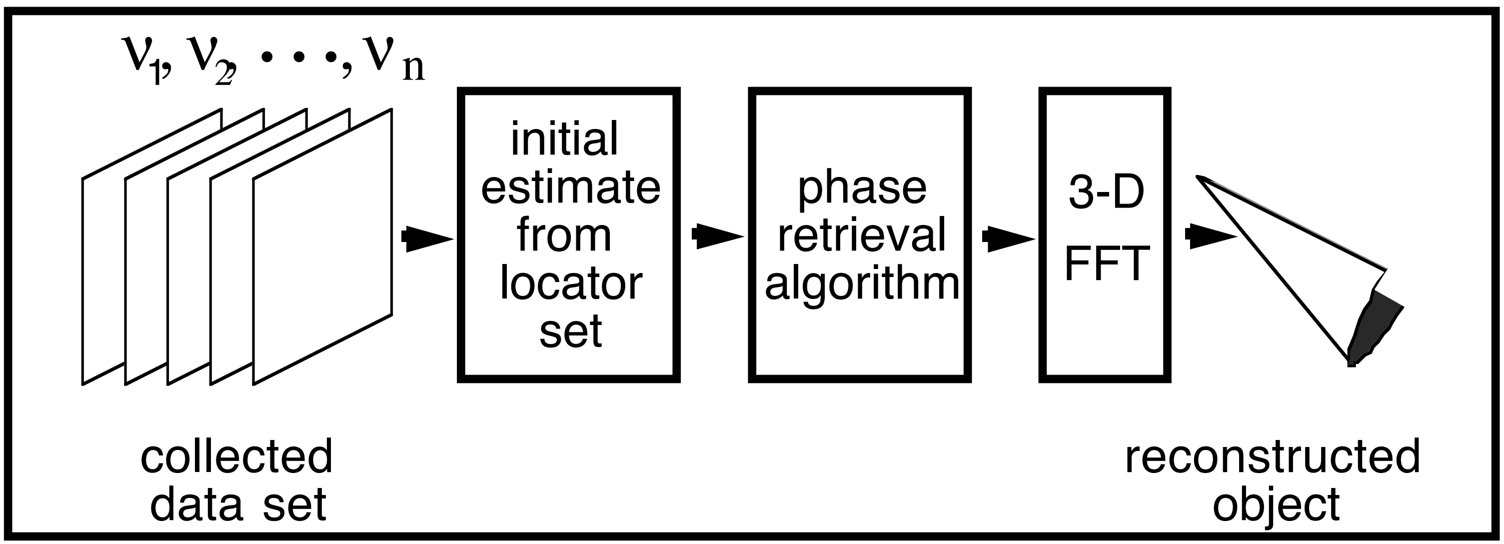

Determine Hubble Space Telescope Aberrations from PSF

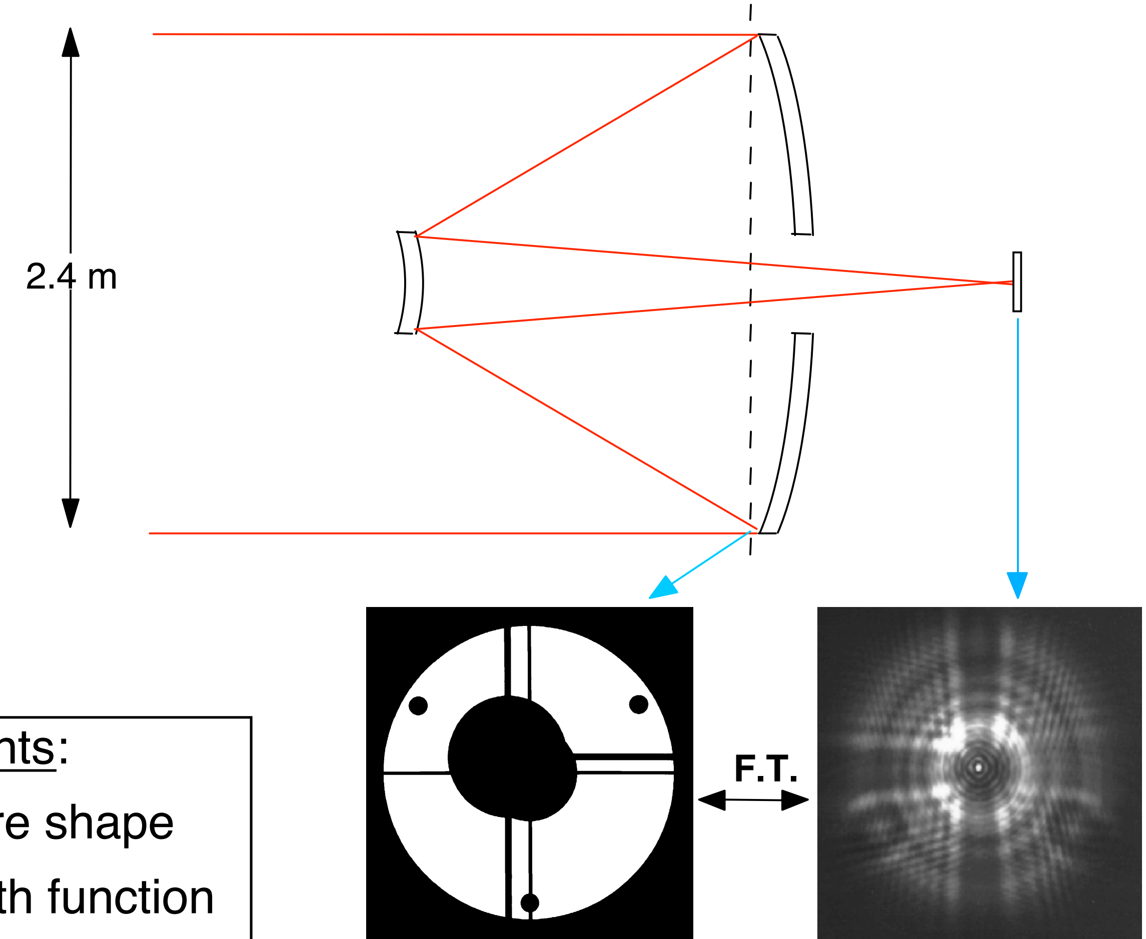

(Hubble Space Telescope)

Measurements & Constraints:

Pupil plane: known aperture shape

phase error fairly smooth function

Focal plane: measured PSF intensity

Wavefronts in pupil plane and focal plane are related by a Fourier Transform

Next Generation Space Telescope
James Webb Space Telescope

- See red-shifted light from early universe
  - 0.6 to 28 µm
  - L2 orbit for passive cooling, avoiding light from sun and earth
  - 6 m diameter primary mirror
    - Deployable, segmented optics
    - Phase retrieval to align segments

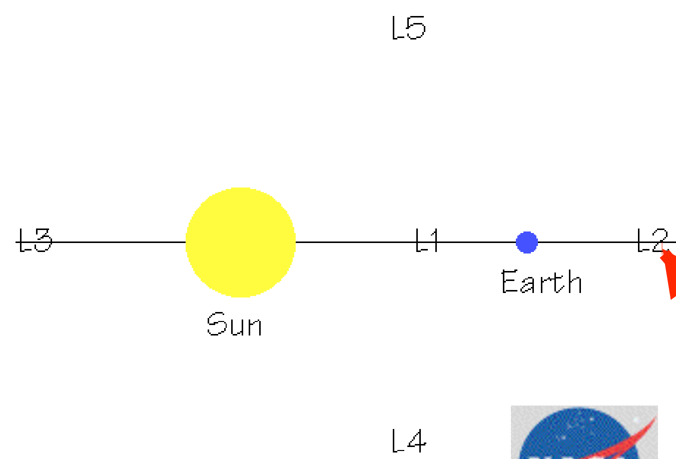

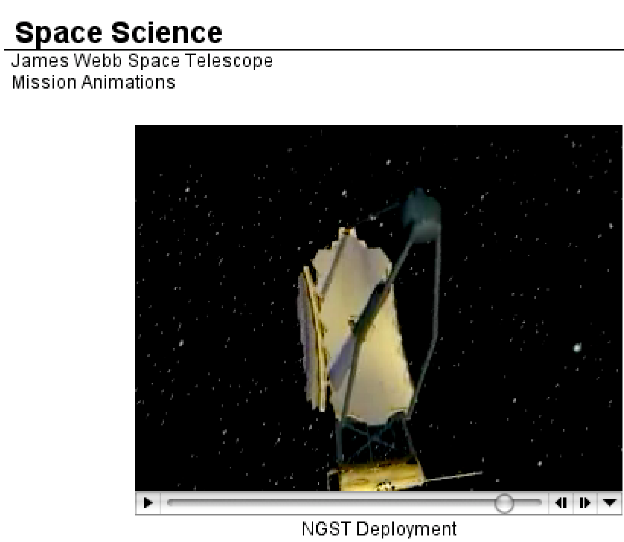

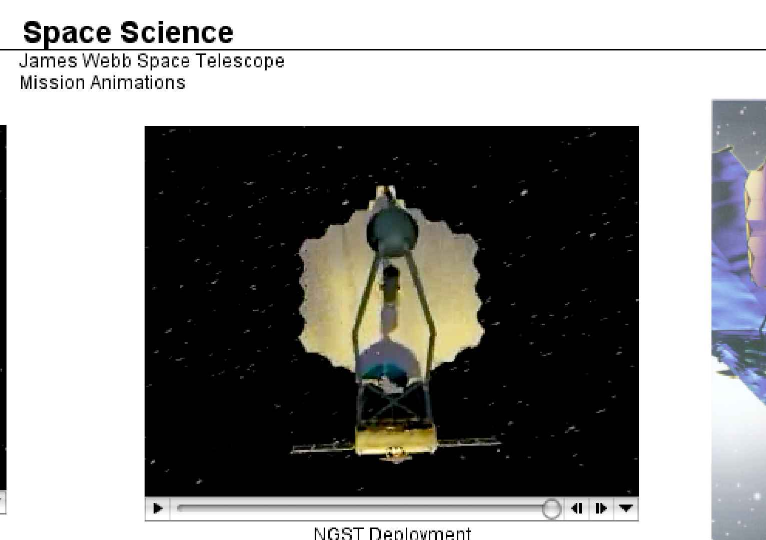

http://ngst.gsfc.nasa.gov/

Optical Testing Using Phase Retrieval

Optical wave fronts (phase) can be measured by many forms of interferometry

<u>Novel wave front sensor:</u> a bare CCD detector array, detects reflected intensity

Wave front reconstructed in the computer by phase retrieval algorithm

Approach:

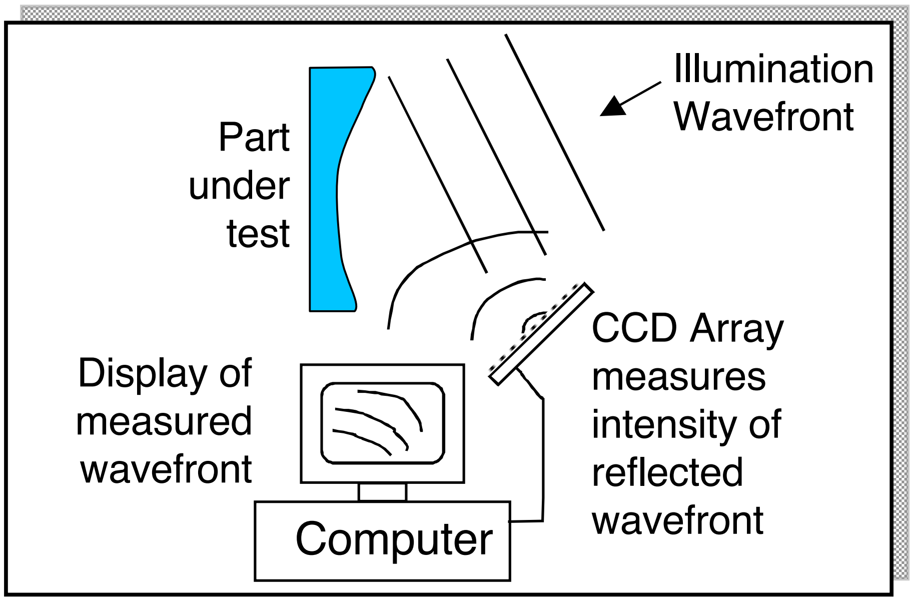

Simulation Results

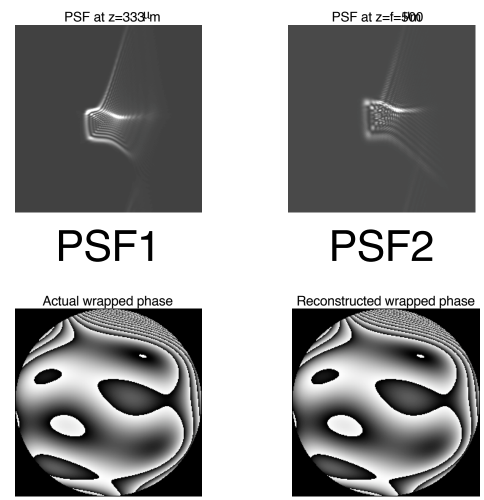

PSF1 PSF2

True Phase Retrieved Phase

Image Reconstruction from X-Ray Diffraction Intensity

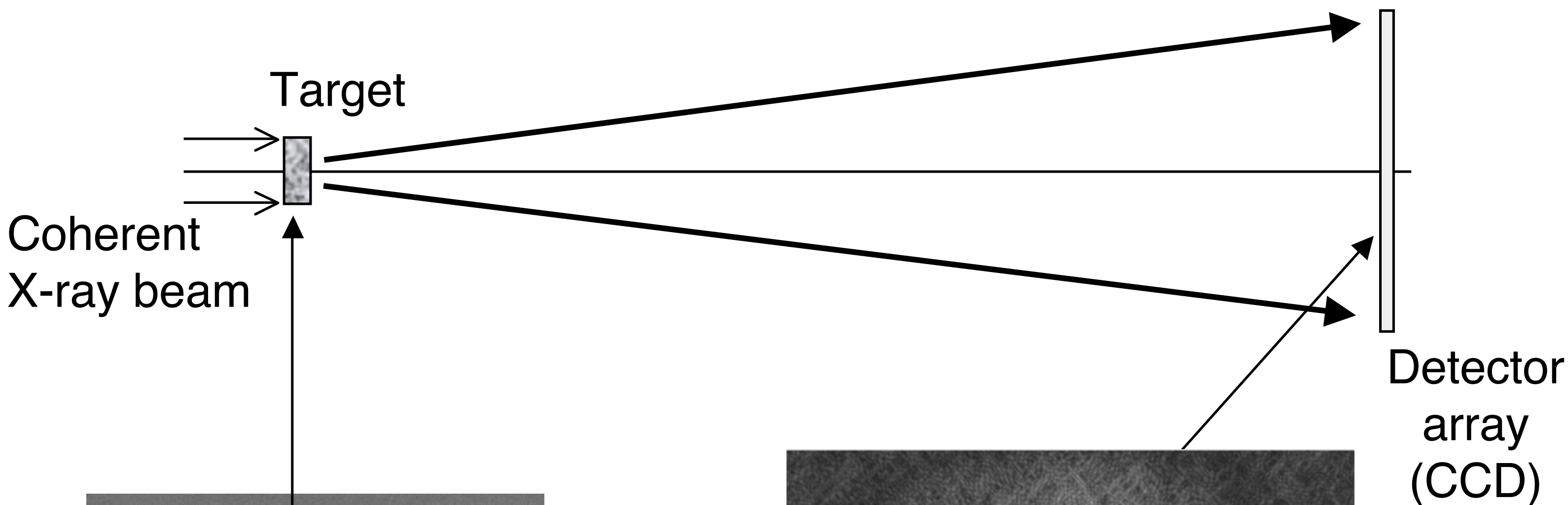

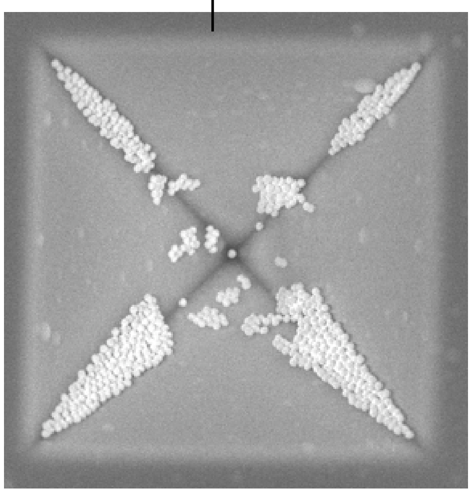

(electron micrograph)
Collection of gold balls
(has complex index of refraction)

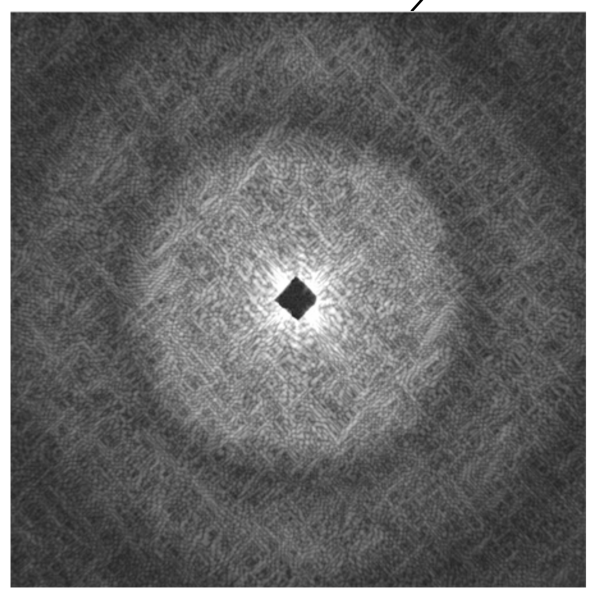

Far-field diffraction pattern
(Fourier intensity)

Phase Retrieval Basics

Fourier transform: $F(u,v) = \int\int_{-\infty}^{\infty} f(x,y) e^{-i2\pi(ux+vy)} dx\,dy$

$$= |F(u,v)| e^{i\psi(u,v)} = \mathcal{F}[f(x,y)]$$

Inverse transform: $f(x,y) = \int\int_{-\infty}^{\infty} F(u,v) e^{i2\pi(ux+vy)} du\,dv = \mathcal{F}^{-1}[F(u,v)]$

Phase retrieval problem:

$$\boxed{\begin{array}{l}\text{Given } |F(u,v)| \text{ and some constraints on } f(x,y),\\ \text{Reconstruct } f(x,y)\text{, or equivalently retrieve } \psi(u,v)\end{array}}$$

$$|F(u,v)| = |\mathcal{F}[f(x,y)]| = \left|\mathcal{F}\left[e^{ic} f(x-x_o, y-y_o)\right]\right| = \left|\mathcal{F}\left[e^{ic} f^*(-x-x_o, -y-y_o)\right]\right|$$

(Inherent ambiguitites: phase constant, images shifts, twin image all result in same data)

Autocorrelation:

$$r_f(x,y) = \int\int_{-\infty}^{\infty} f(x',y') f^*(x'-x, y'-y) dx'dy' = \mathcal{F}^{-1}\left[|F(u,v)|^2\right]$$

- Patterson function in crystallography is an aliased version of the autocorrelation
- Simply need Nyquist sampling of the Fourier intensity to avoid aliasing

Autocorrelation versus Patterson Function

Autocorrelation:

$$r_f(x,y) = \int\int_{-\infty}^{\infty} f(x',y')f^*(x'-x,y'-y)dx'dy' = \mathcal{F}^{-1}\left[\left|F(u,v)\right|^2\right]$$

has all vector separations in object

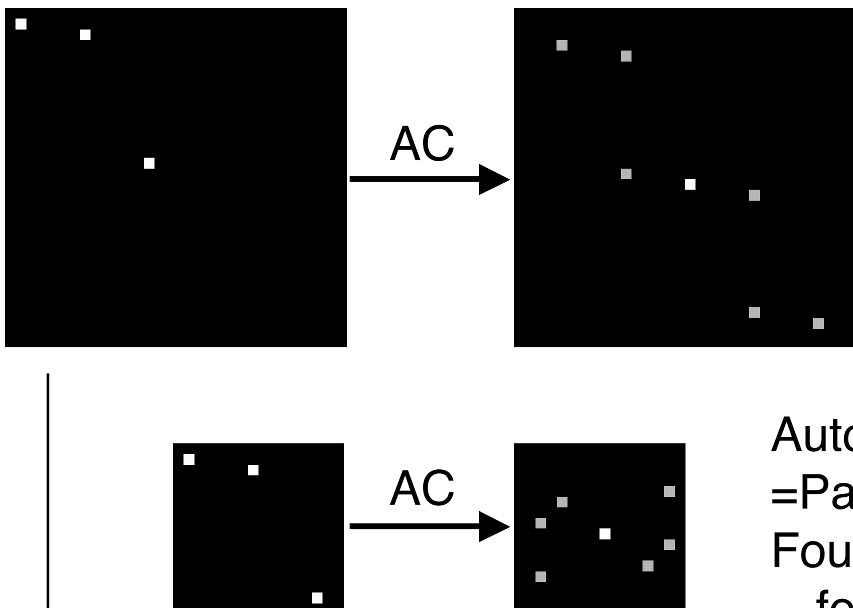

(unit cell)

Autocorrelation Function:
Fourier intensities adequately (Nyquist) sampled or oversampled
NO Aliasing $\Delta u \leq \lambda z/(2D_u)$

Autocorrelation Function
=Patterson function
Fourier intensities <u>undersampled</u>
-- forced by crystallographic periodicity
Get Aliasing $\Delta u = \lambda z/D_u > \lambda z/(2D_u)$

If in repeated array,
Object embedded
in zeros by factor of 2

In repeated array,
Object NOT embedded
in zeros by factor of 2

Constraints in Phase Retrieval

- Nonnegativity constraint: $f(x, y) \geq 0$
  - True for ordinary incoherent imaging, crystallography, MRI, etc.
  - Not true for wavefront sensing or coherent imaging (sometimes x-ray)

- The <u>support</u> of an object is the set of points over which it is nonzero
  - Meaningful for imaging objects on dark backgrounds
  - Wavefront sensing through a known aperture

- A good support constraint is essential for complex-valued objects
  - Coherent imaging or wave front sensing

- Atomiticity when have angstrom-level resolution
  - For crystals -- <u>not</u> applicable for coarser-resolution, single-particle

- Object intensity constraint (wish to reconstruct object phase)
  - E.g., measure wavefront intensity in two planes (Gerchberg-Saxton)
  - If available, supercedes support constraint

First Phase Retrieval Result

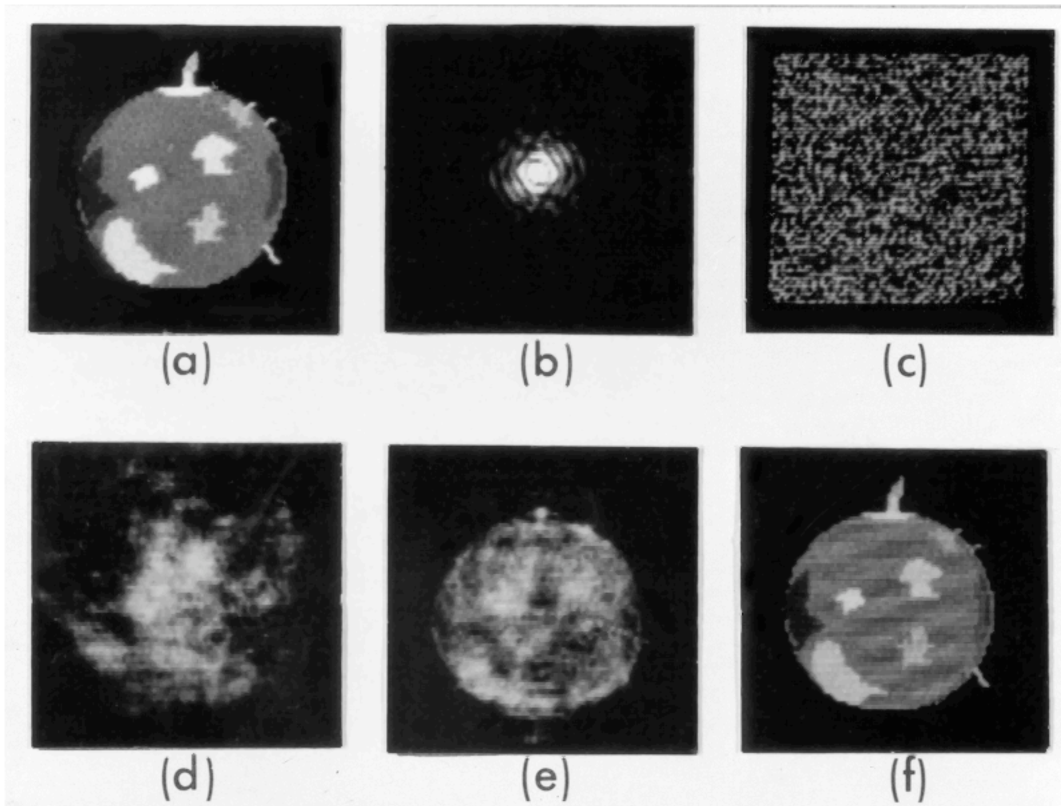

(a) Original object, (b) Fourier modulus data, (c) Initial estimate
(d) – (f) Reconstructed images — number of iterations: (d) 20, (e) 230, (f) 600

Reference: J.R. Fienup, Optics Letters, Vol 3., pp. 27-29 (1978).

Iterative Transform Algorithm

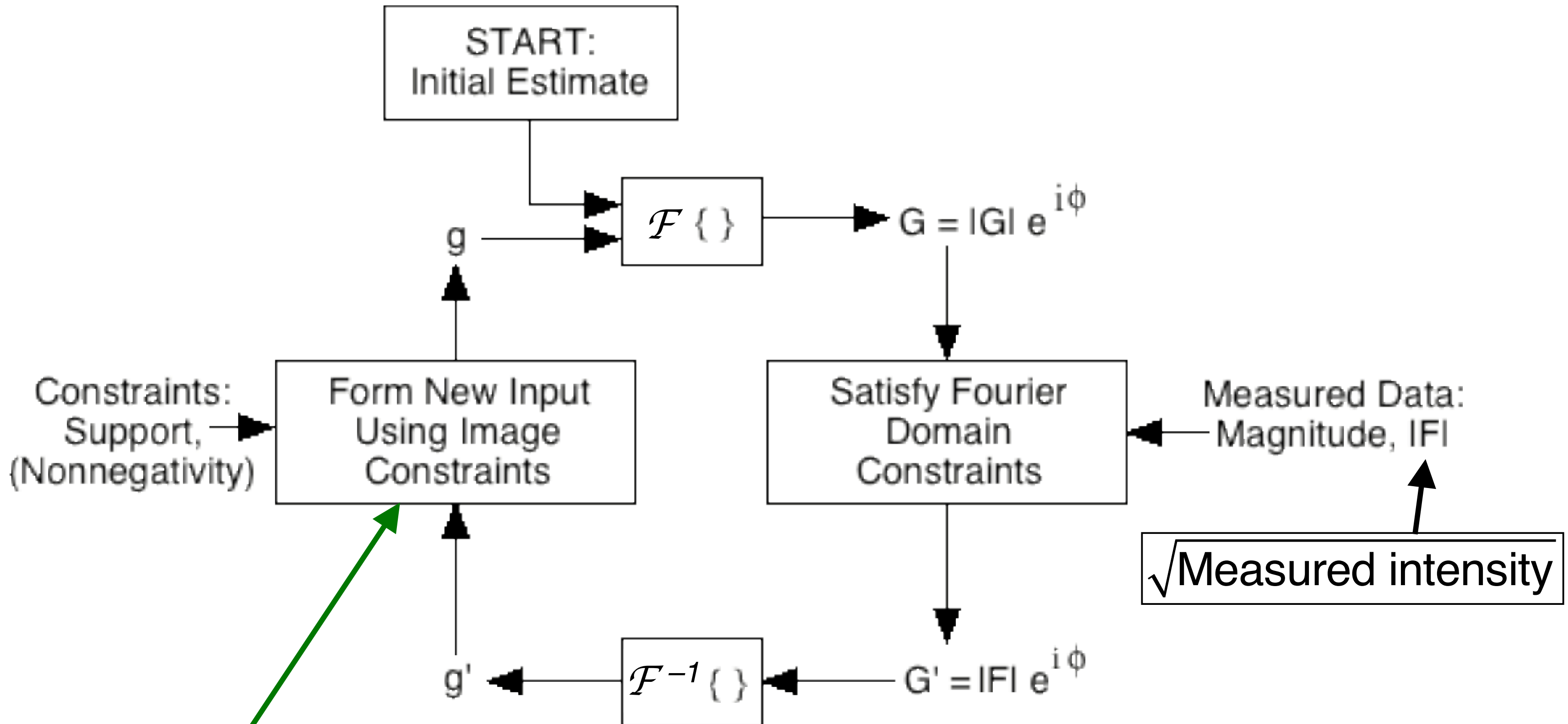

Hybrid Input-Output version

$$g_{k+1}(x,y)=\begin{cases} g'_k(x,y) & ,\ (x,y)\in \text{ Support}\\ g_k(x,y)-\beta g'_k(x,y), & (x,y)\notin \text{ Support}\end{cases}$$

Iterative Transform Algorithm Versions: Error-Reduction versus HIO

- Error reduction algorithm ER: $g_{k+1}(x) = \begin{cases} g'_k(x)\ , & x \in S \ \&\ g'_k(x) \geq 0 \\ 0\ , & \text{otherwise} \end{cases}$
  - Satisfy constraints in object domain
  - Equivalent to projection onto (nonconvex) sets algorithm
  - Equivalent to successive approximations
  - Similar to steepest-descent gradient search
  - Proof of convergence (weak sense)
  - In practice: slow, prone to stagnation, gets trapped in local minima
- Hybrid-input-output algorithm HIO: $g_{k+1}(x) = \begin{cases} g'_k(x)\ , & x \in S \ \&\ g'_k(x) \geq 0 \\ g_k(x) - \beta g'_k(x)\ , & \text{otherwise} \end{cases}$
  - Uses negative feedback idea from control theory
    - β is feedback constant
  - No convergence proof (can increase errors temporarily)
  - In practice: much faster than ER
  - Can climb out of local minima at which ER stagnates

Image Reconstruction from Simulated Speckle Interferometry Data

Labeyrie's stellar speckle interferometry gives this

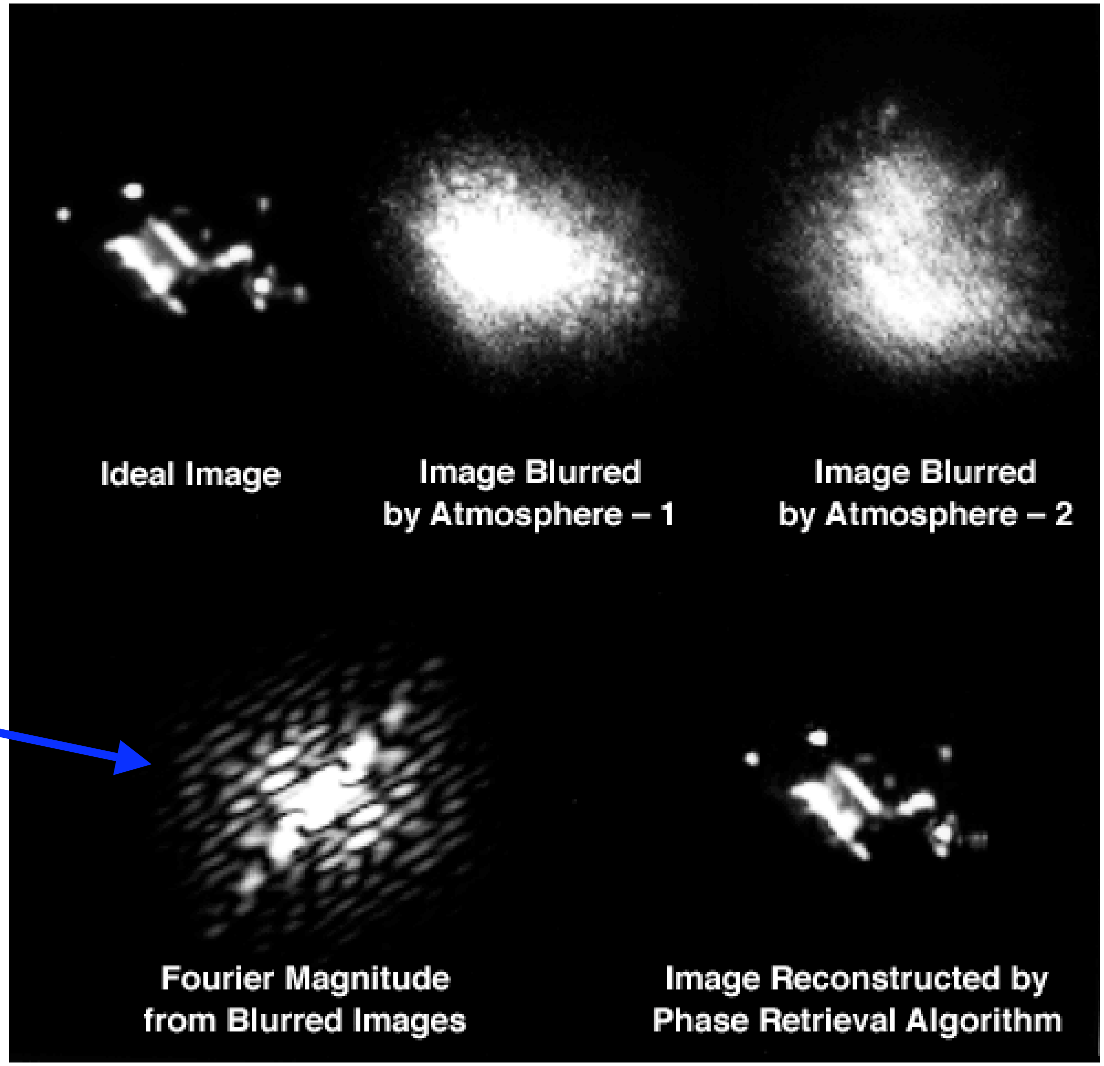

J.R. Fienup, "Phase Retrieval Algorithms: A Comparison," Appl. Opt. <u>2l</u>, 2758-2769 (1982).

Error Metric versus Iteration Number

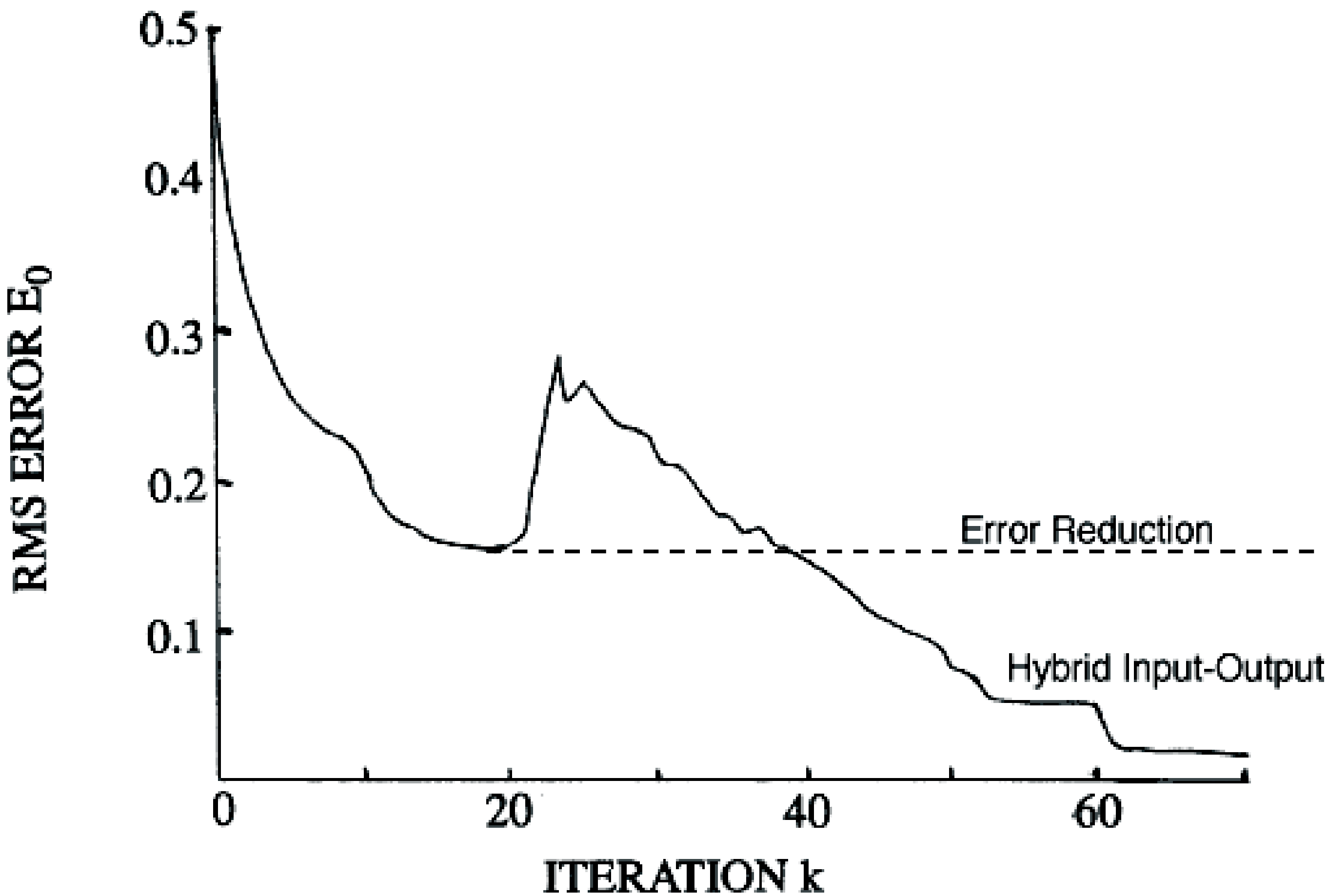

Nonlinear Optimization Algorithms Employing Gradients

Minimize Error Metric, e.g.: $E = \sum_u W(u)[|G(u)| - |F(u)|]^2$

Contour Plot of Error Metric

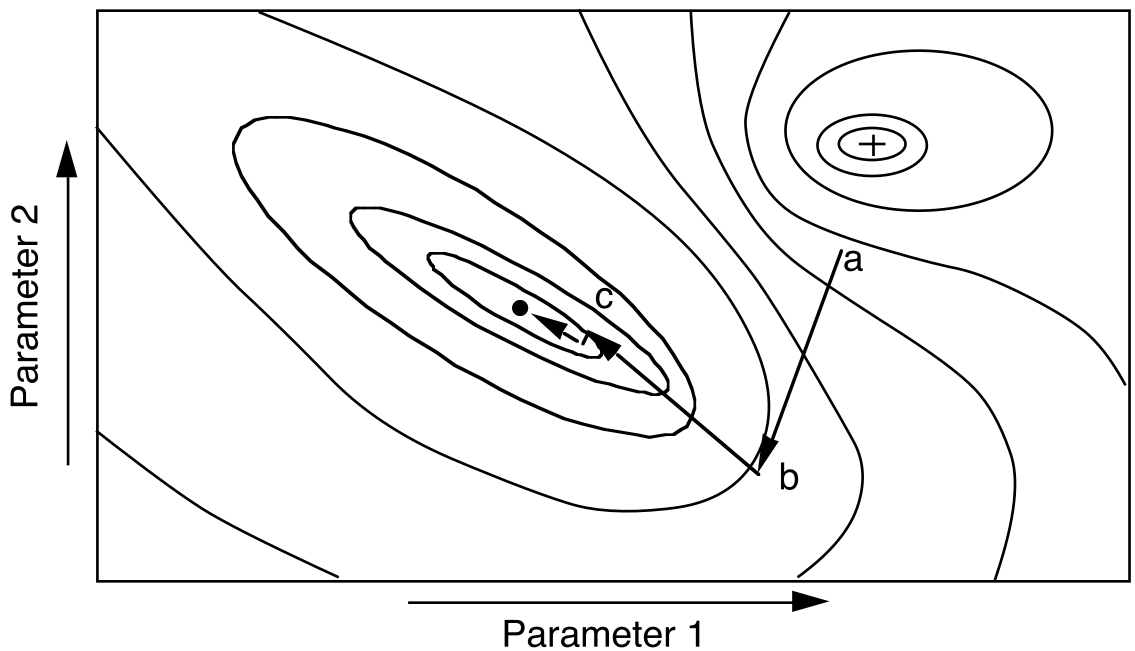

Repeat three steps:

1. Compute gradient: $\frac{\partial E}{\partial p_1}, \frac{\partial E}{\partial p_2}, \ldots$
2. Compute direction of search
3. Perform line search

Gradient methods:

(Steepest Descent)
Conjugate Gradient
BFGS/Quasi-Newton
…

Analytic Gradients with Phase Values as Parameters

$$\boxed{E = \sum_u W(u)\left[|G(u)| - |F(u)|\right]^2} \qquad G(u) = \mathcal{P}\left[g(x)\right]$$

Optimizing over $g(x) = g_R(x) + i\, g_I(x) = m_o(x)\, e^{i\theta(x)}$, $\theta(x) = \sum_{j=1}^{J} a_j Z_j(x)$

For point-by-point pixel (complex) value, $g(x)$, $\dfrac{\partial E}{\partial g(x)} = 2\ \mathrm{Im}\left\{ g^{W*}(x) \right\}$

For point-by-point phase map, $\theta(x)$, $\dfrac{\partial E}{\partial \theta(x)} = 2\ \mathrm{Im}\left\{ g(x)\, g^{W*}(x) \right\}$

For Zernike polynomial coefficients, $\dfrac{\partial E}{\partial a_j} = 2\ \mathrm{Im}\left\{ \sum_x g(x)\, g^{W*}(x) Z_j(x) \right\}$

where

$$G^W(u) = W(u)\left[|F(u)| \frac{G(u)}{|F(u)|} - G(u) \right], \text{ and } g^W(x) = \mathcal{P}^{\dagger}\left[G^W(u) \right]$$

$\mathcal{P}[\bullet]$ can be a single FFT or multiple-plane Fresnel transforms with phase factors and obscurations

Analytic gradients very fast compared with calculation by finite differences

J.R. Fienup, "Phase-Retrieval Algorithms for a Complicated Optical System," Appl. Opt. 32, 1737-1746 (1993).

J.R. Fienup, J.C. Marron, T.J. Schulz and J.H. Seldin, "Hubble Space Telescope Characterized by Using Phase Retrieval Algorithms," Appl. Opt. 32 1747-1768 (1993).

Support Constraints

Example of Algorithm for Deriving Bounds on Object Support

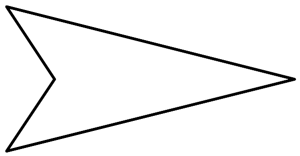

Object Support S

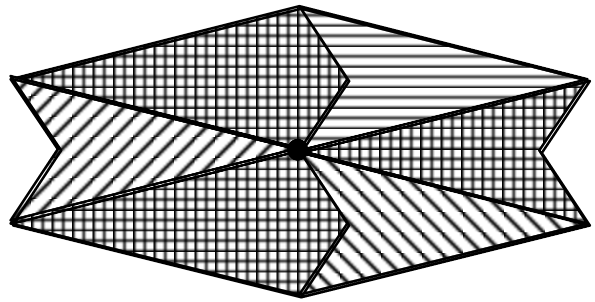

Forming Autocorrelation Support

$$A = S - S \equiv \{x - y : x, y \in S\}$$

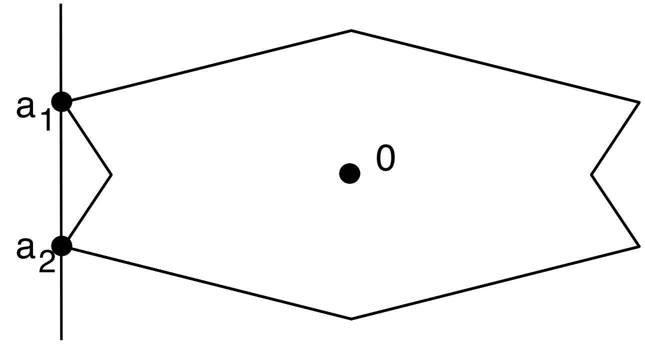

Autocorrelation Support

$a_1, a_2 \ldots$ are "extreme points" they must all be contained in one translate of the object, S

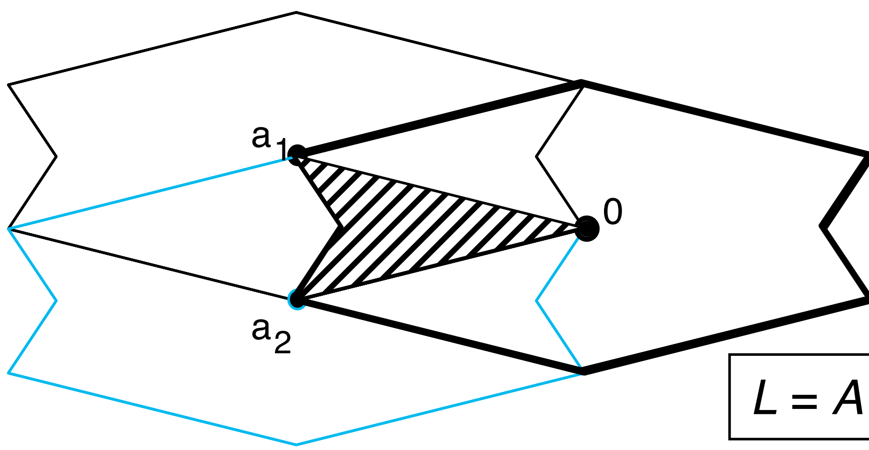

$$L = A \cap (A + a_1) \cap (A + a_2) \cap \ldots$$

Triple Intersection of Autocorrelation Supports

Triple-Intersection Rule: [Crimmins, Fienup, & Thelen, JOSA A **7**, 3 (1990)]

The Institute of OPTICS

Triple Intersection for Triangle Object

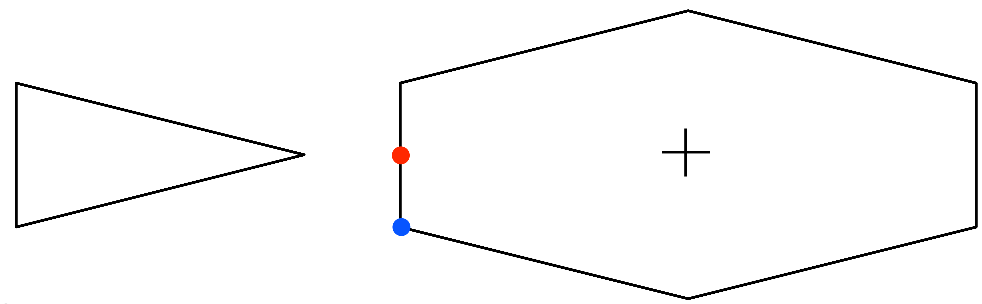

Object Support

Autocorrelation Support

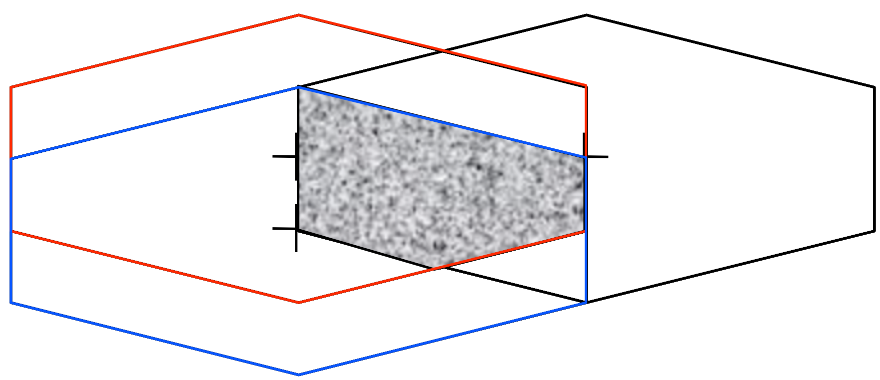

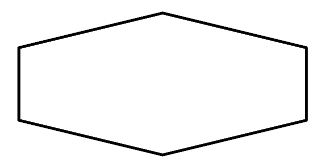

Alternative Object Support

Triple Intersection – Support Constraint

- Family of solutions for object support from autocorrelation support
- Use upper bound for support constraint in phase retrieval

Triple Intersection for Collections of Points

Vol. 72, No. 5/May 1982/J. Opt. Soc. Am. 615

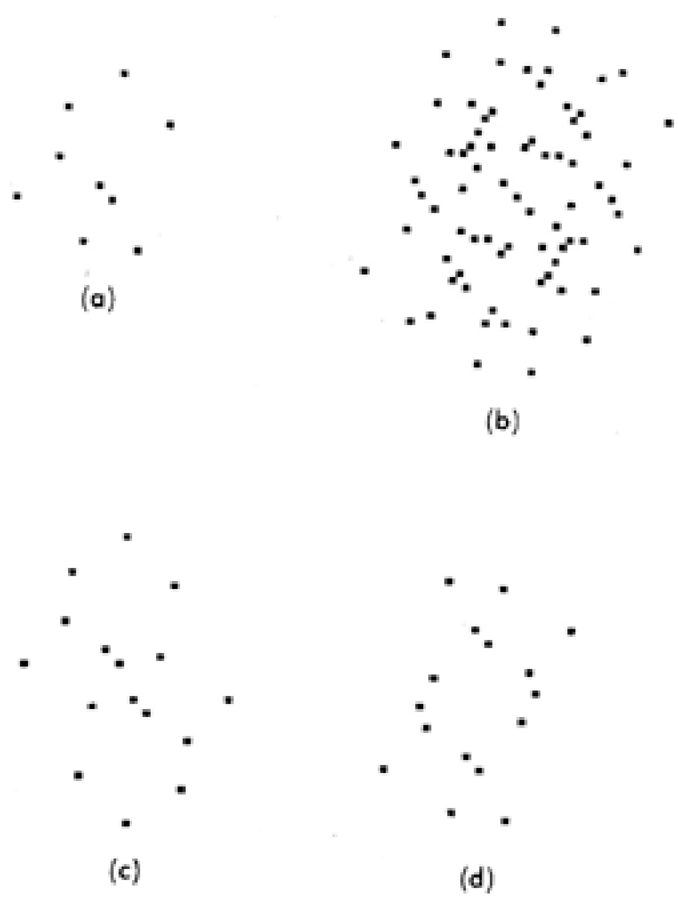

Fig. 7. Autocorrelation tri-intersection for sets consisting of a collection of distinct points. (a) Set S, (b) $A = S - S$, (c) and (d) locators of the form $L = A \cap (w + A)$. Intersecting (c) or (d) with (b) yields the unique solution (a).

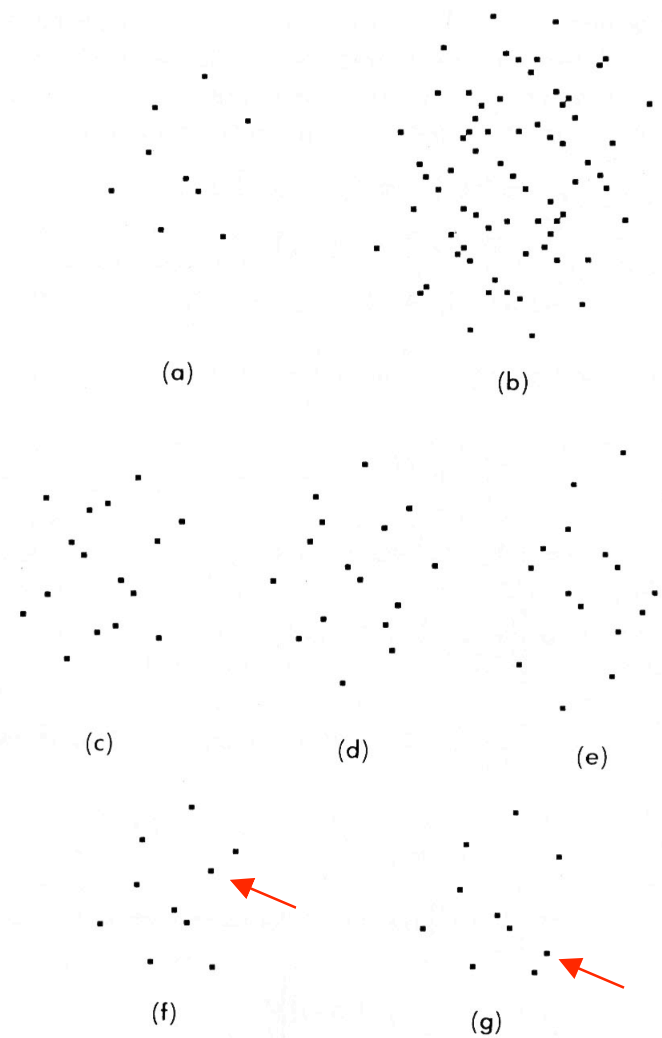

Fig. 8. Autocorrelation intersection for redundant case. (a) Set S, (b) $A = S - S$, (c)–(e) locators of the form $L = A \cap (w + A)$, (f) intersection of (c) with (d), (g) another intersection of three translates of A.

Arrangements of Points Preventing Triple Intersection

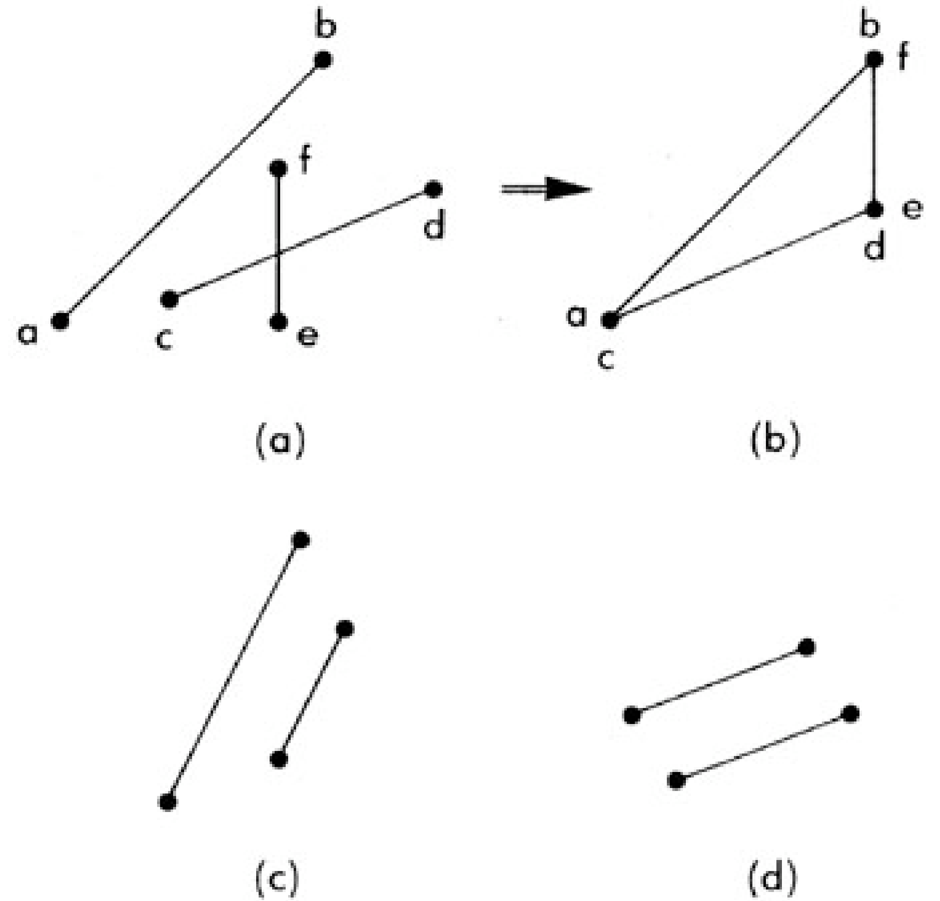

Fig. 9. Redundancy types of relationships within S that would violate Condition 1. (a) and (b) three vector separations add to zero, (c) one vector separation is twice another, (d) two vector separations are equal.

Reconstruction of Values of Collection of Points

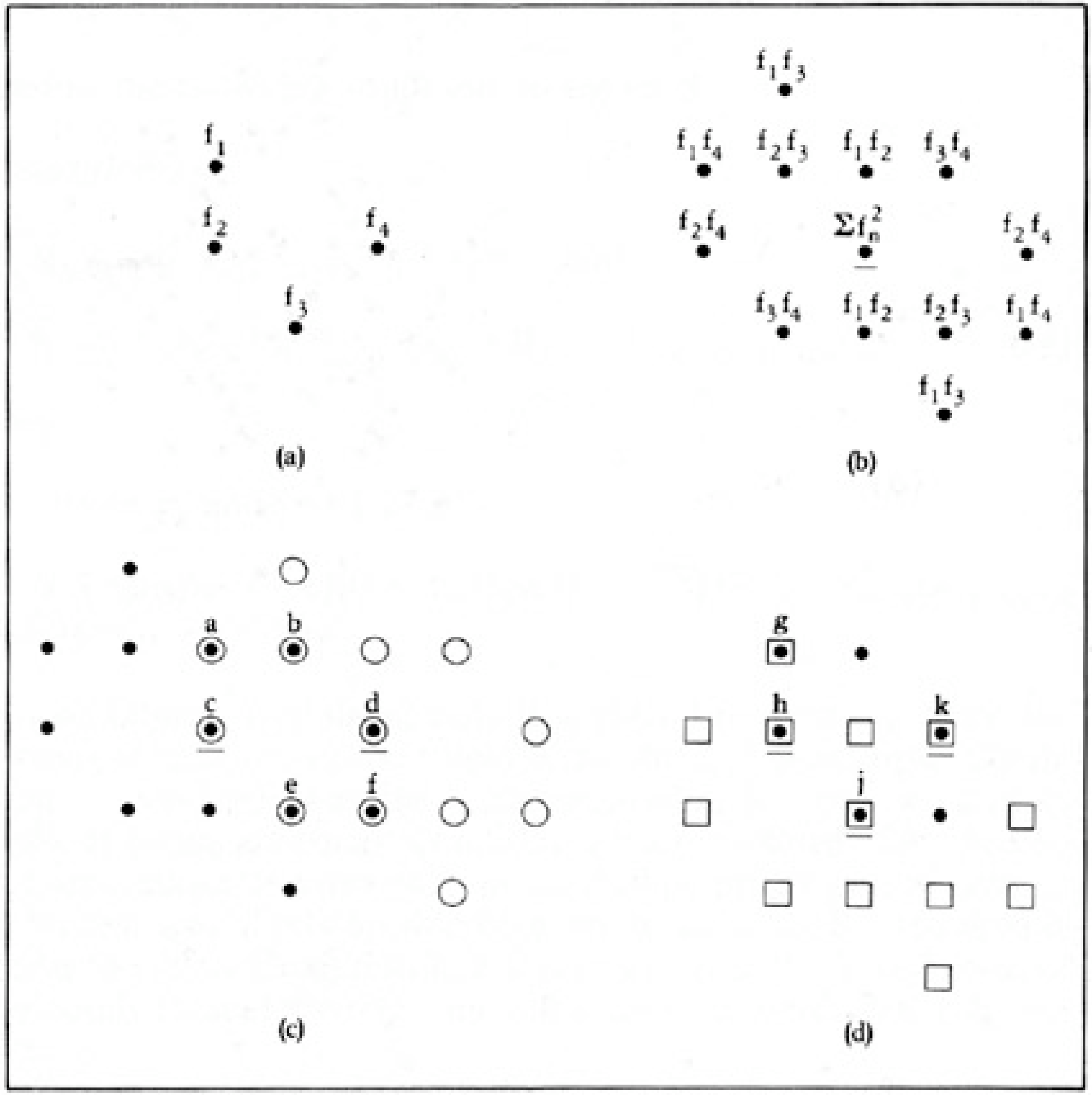

Autocorrelation Support

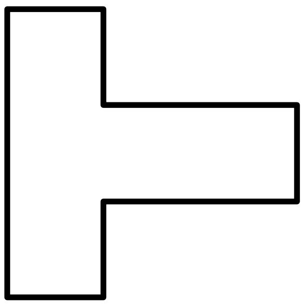

Object
Support

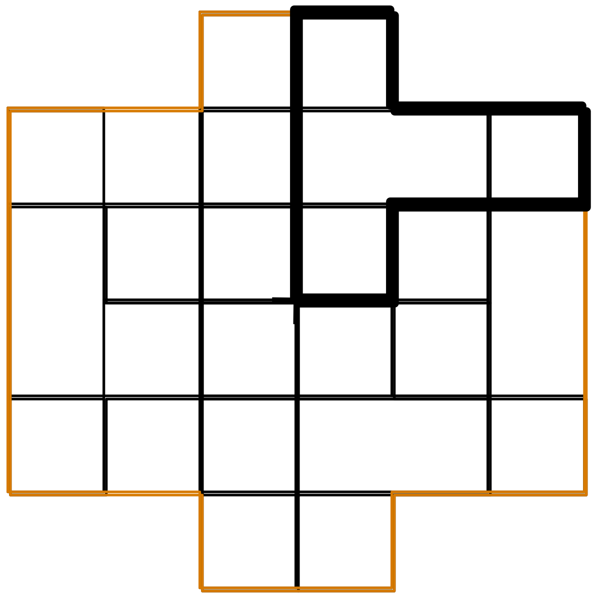

Forming the
Autocorrelation
Support

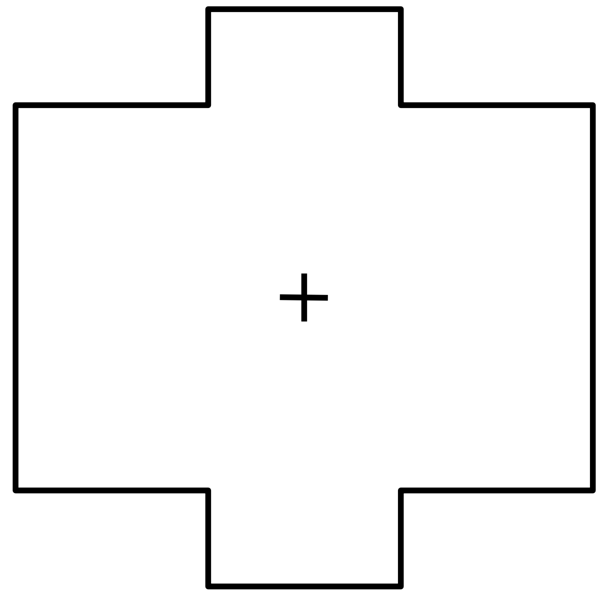

Autocorrelation
Support

Locator Sets

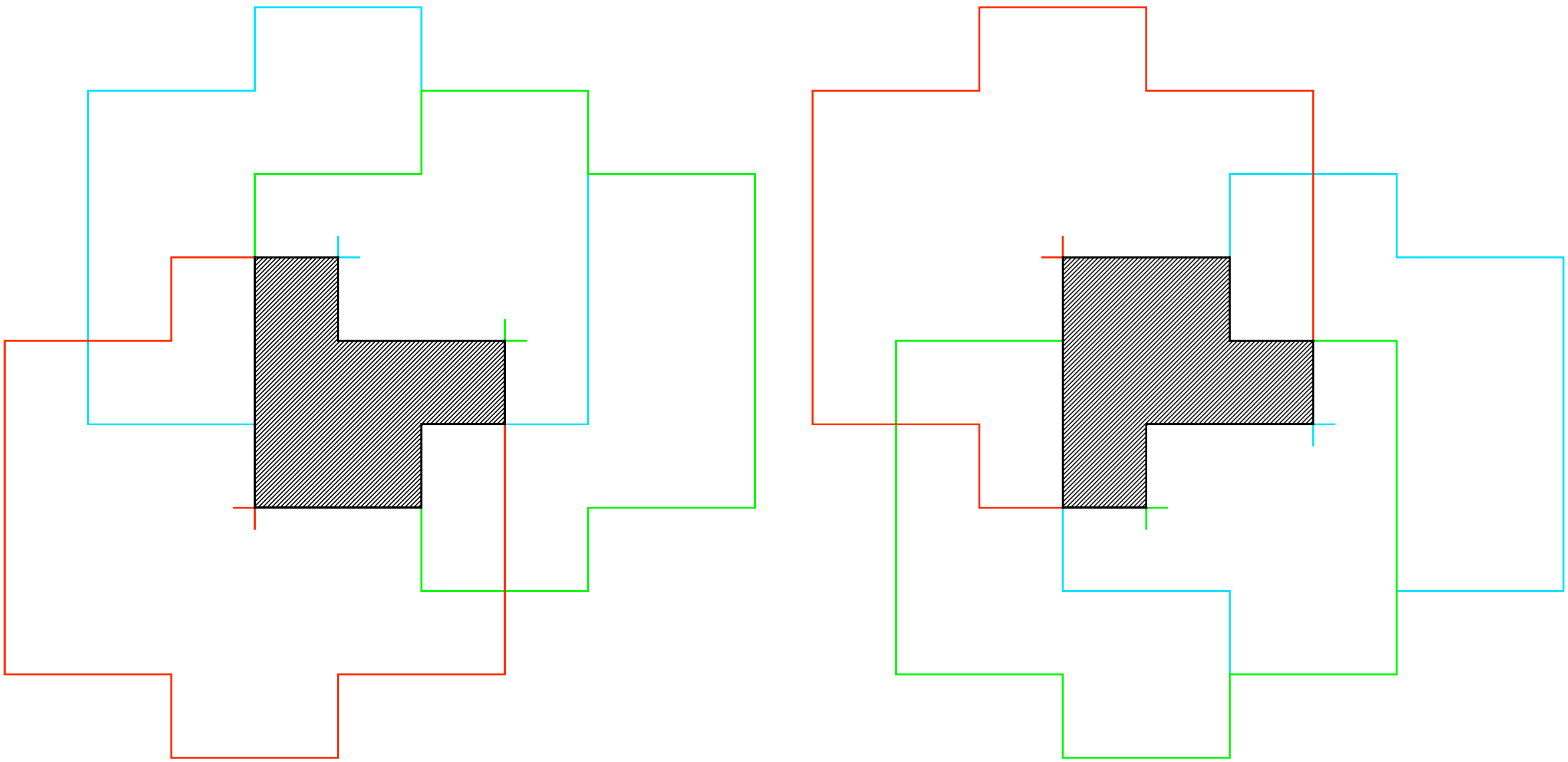

Triple intersection rule

Includes all possible object supports that give rise to autocorrelation support

Combination of Locator Sets

- Must be able to restrict alignment horizontally and vertically,
  - if half the autocorrelation width in each dimension and determine whether have twinned locator set

- Then align and intersect locator sets to arrive at smaller (better) locator set

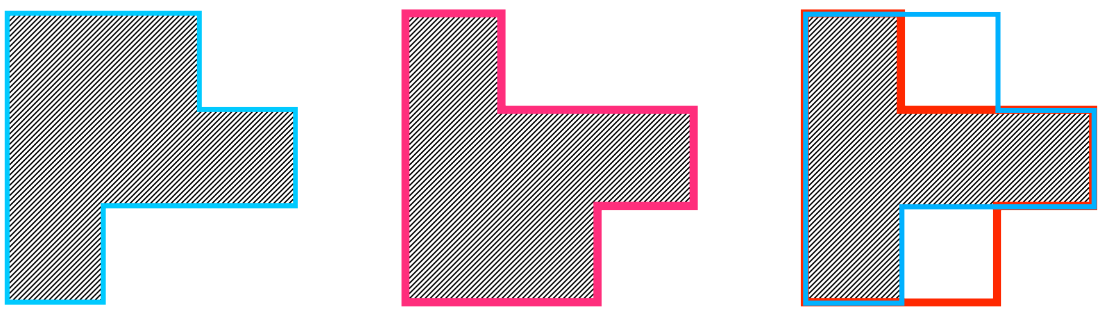

Binary Object Example

Object

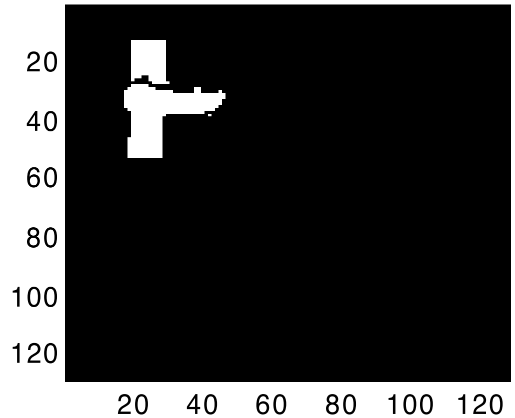

Autocorrelation (not binary)

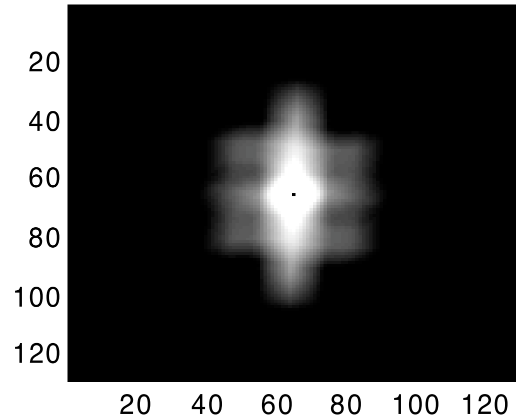

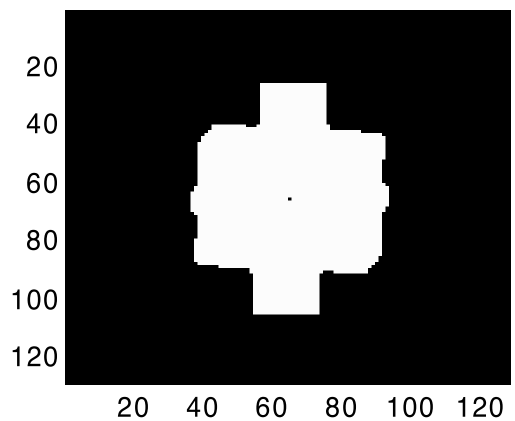

Thresholded Autocorrelation
(Estimated Autocorrelation Support)

Finding Vertex Points on Autocorrelation Support

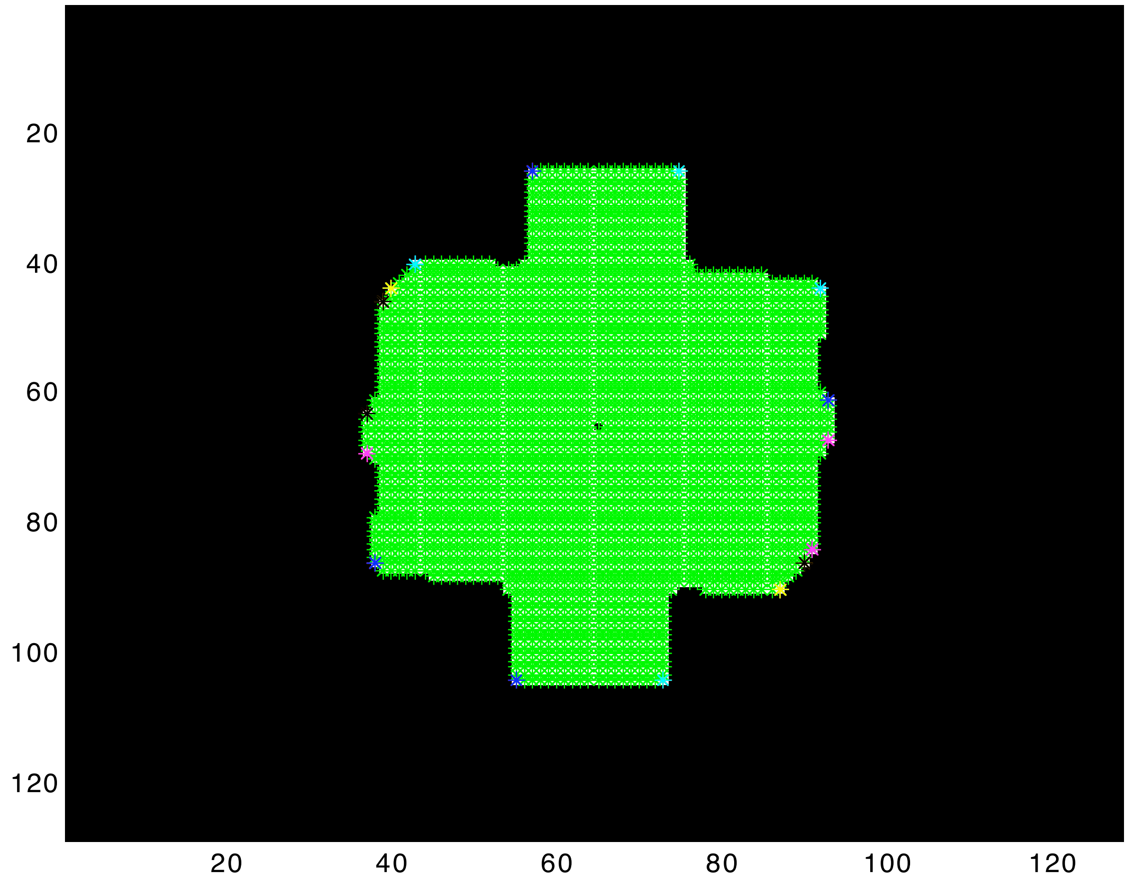

(Use Vertex Points for Triple Intersection)

3 Locator Sets and a Combination of Them

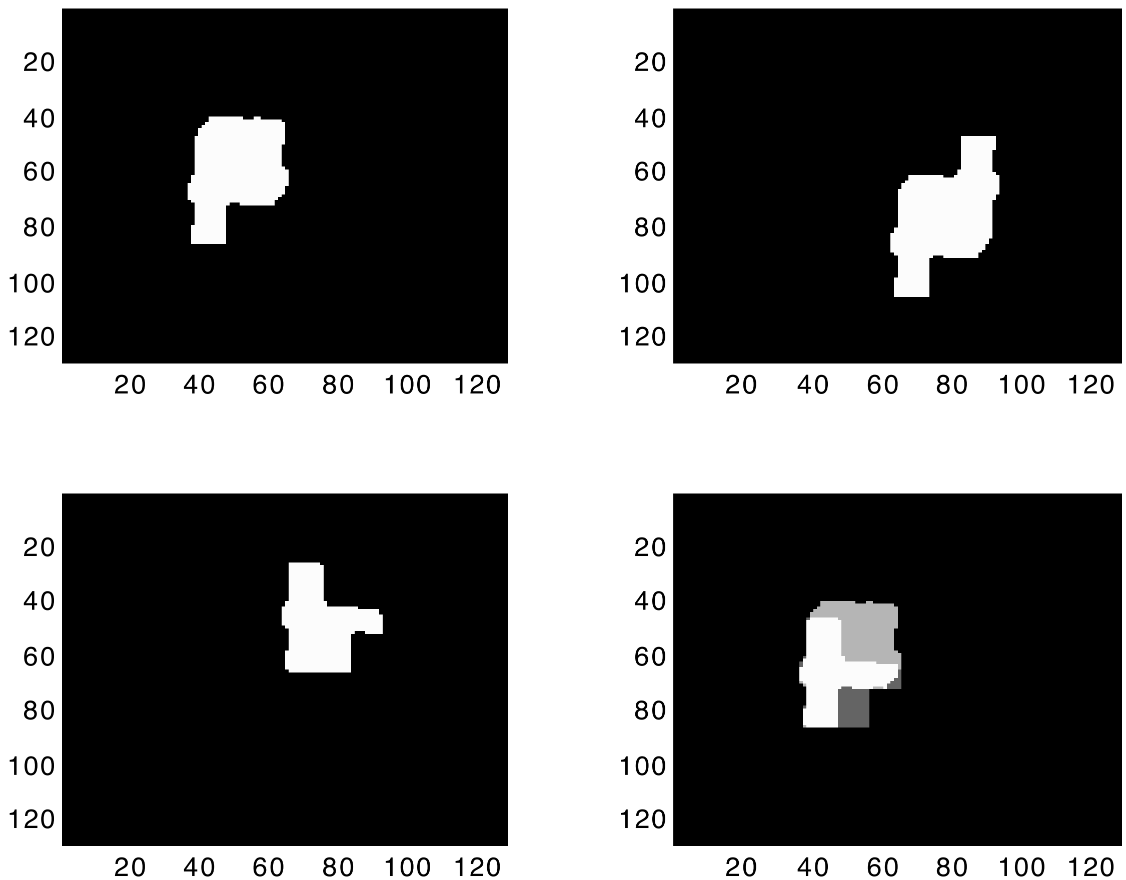

Gray-Level Object Example

Object

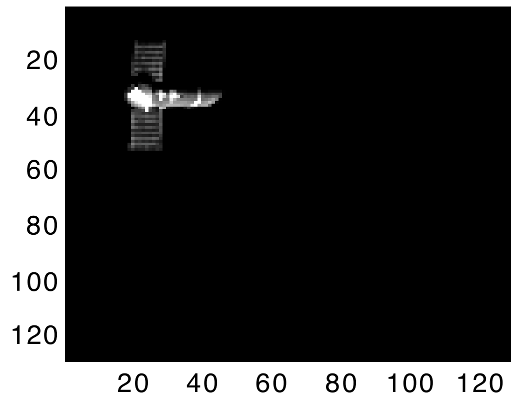

Autocorrelation

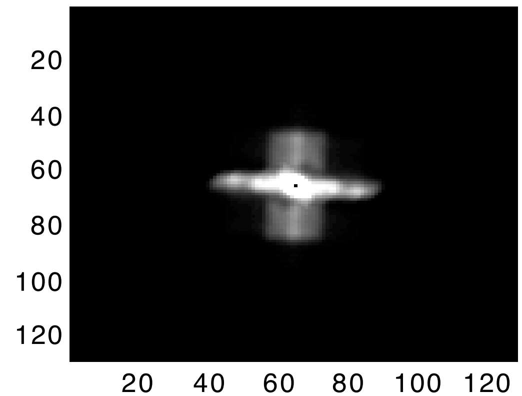

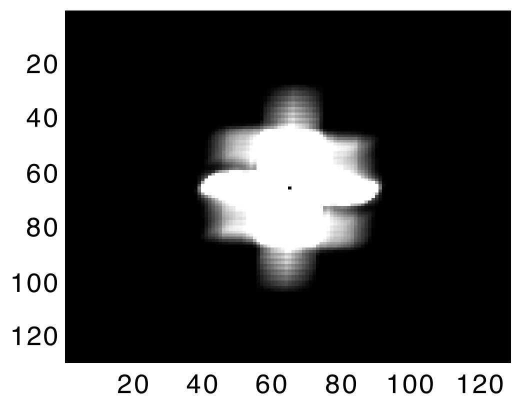

Autocorrelation
(highly overexposed)

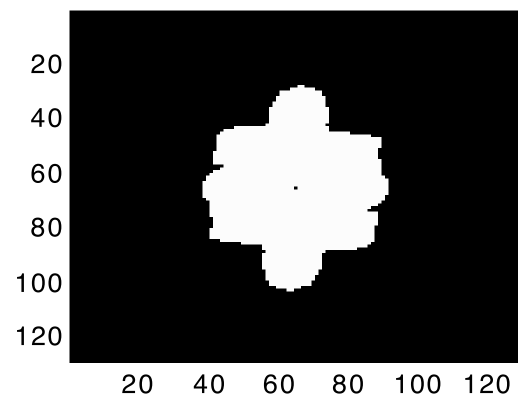

Thresholded
Autocorrelation

Finding Vertex Points on Autocorrelation Support

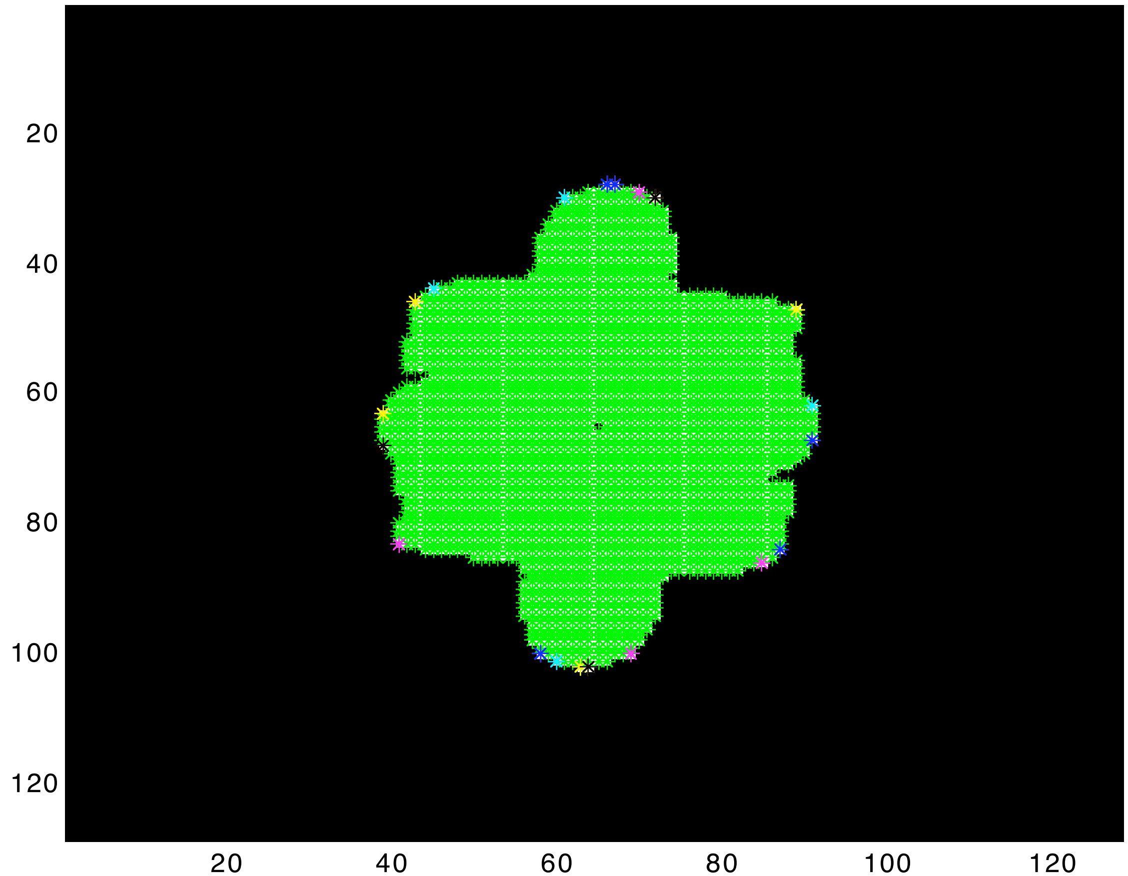

Use Vertex Points for Triple Intersection

2 Locator Sets and a Combination

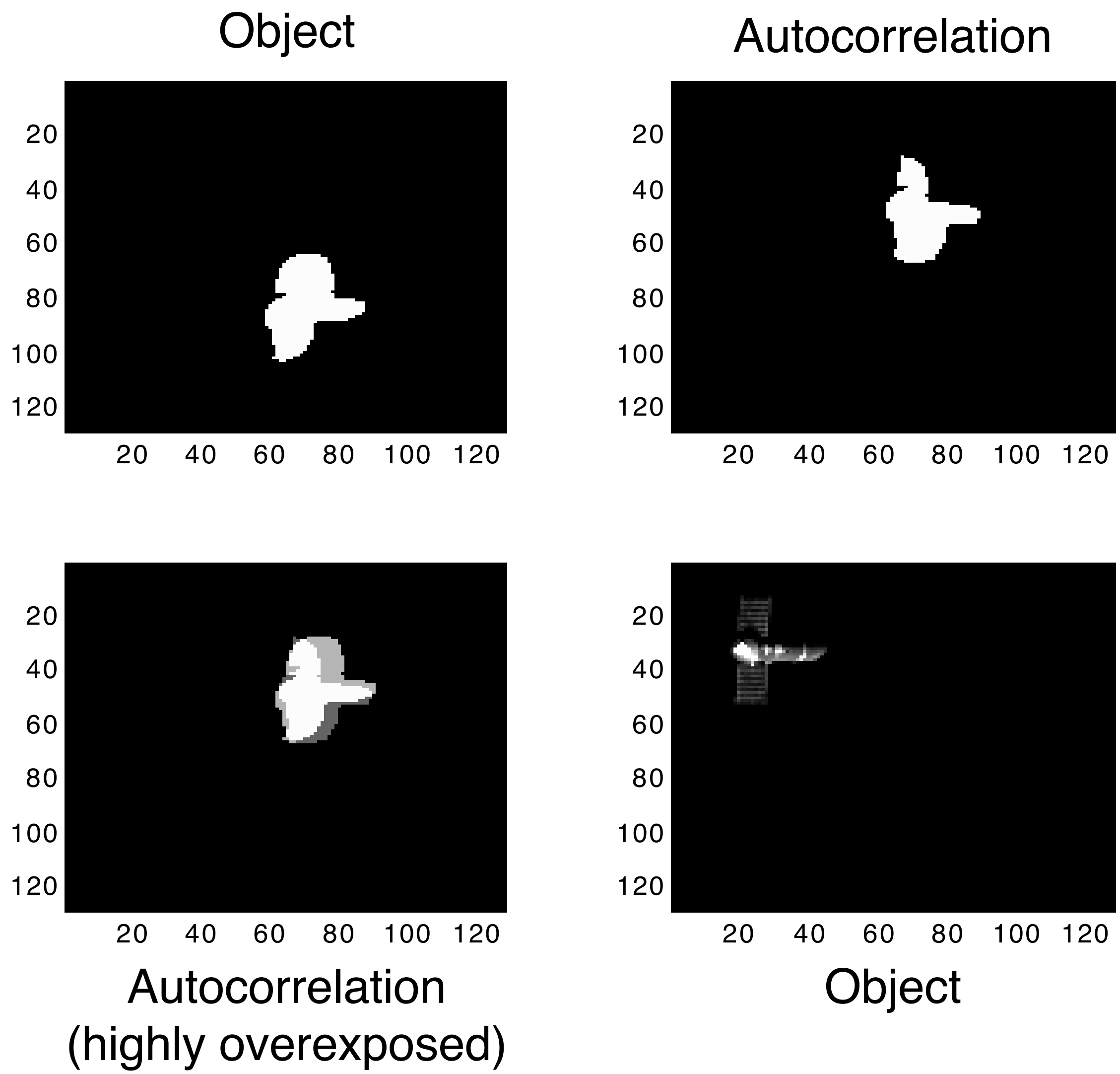

Object for Laboratory Experiments

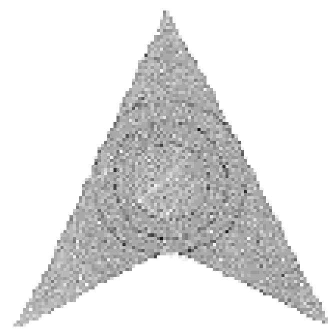

ST Object. The three concentric discs forming a pyramid can be seen as dark circles at their edges. The small piece on one of the two lower legs was removed before this photograph was taken.

PROCLAIM 3-D Imaging Concept

Phase Retrieval with Opacity Constraint LAser IMaging

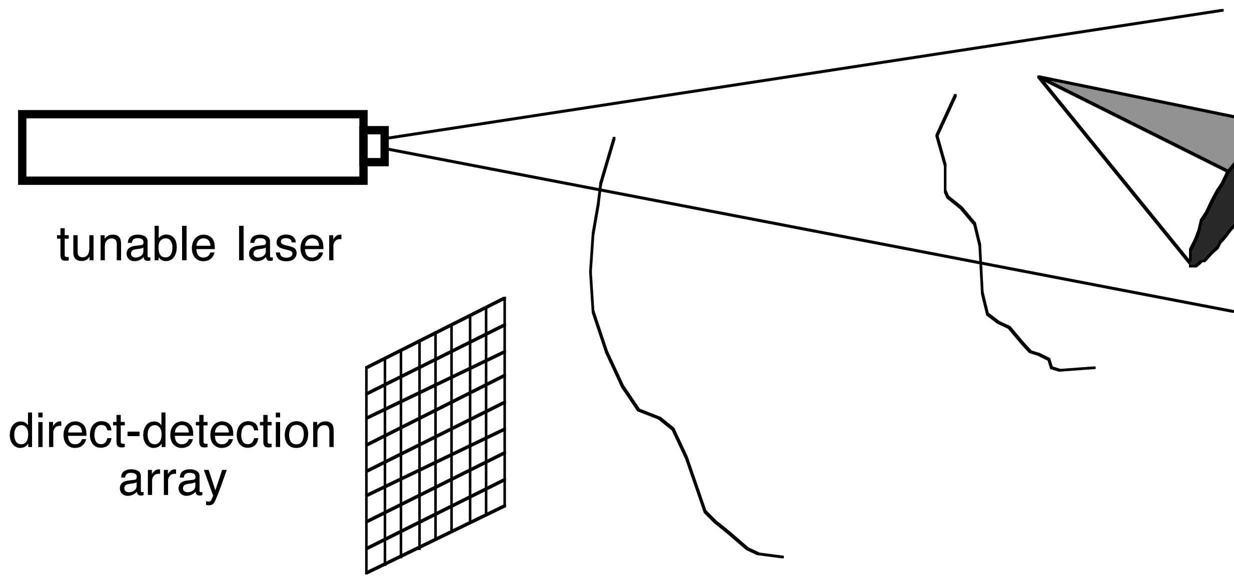

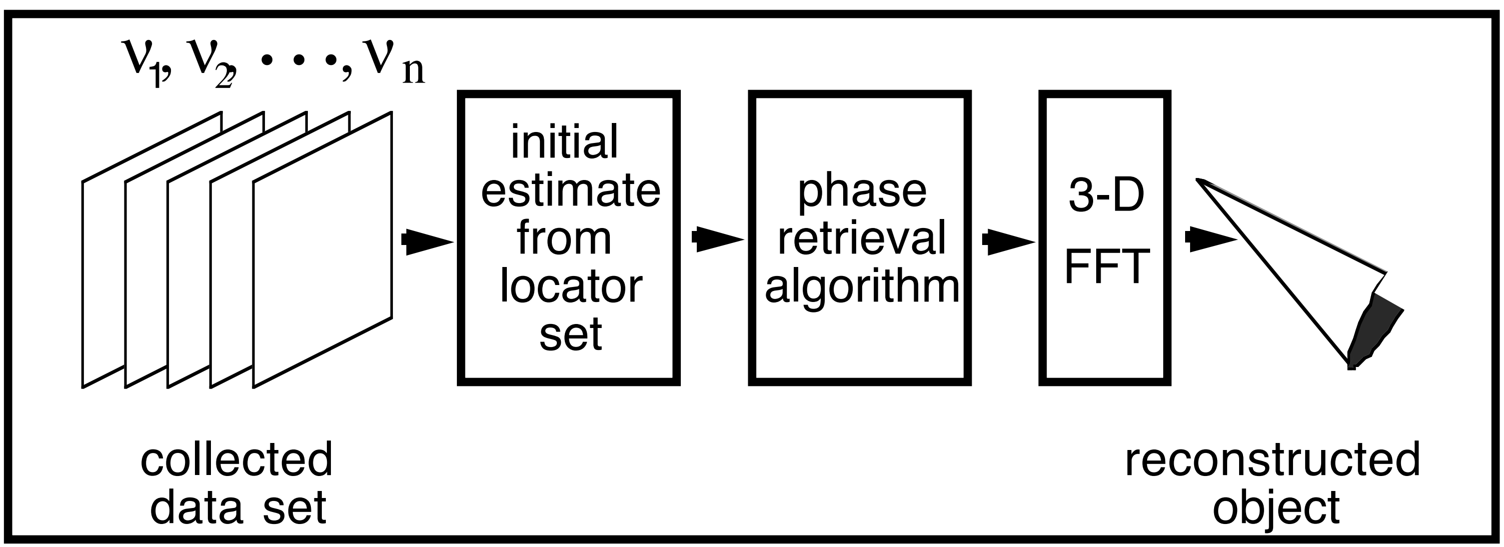

3-D Laser Fourier Intensity Laboratory Data

Data cube:

1024x1024 CCD pixels
x 64 wavelengths

Shown at right:
128x128x64 sub-cube

(128x128 CCD pixels at each of 64 wavelengths)

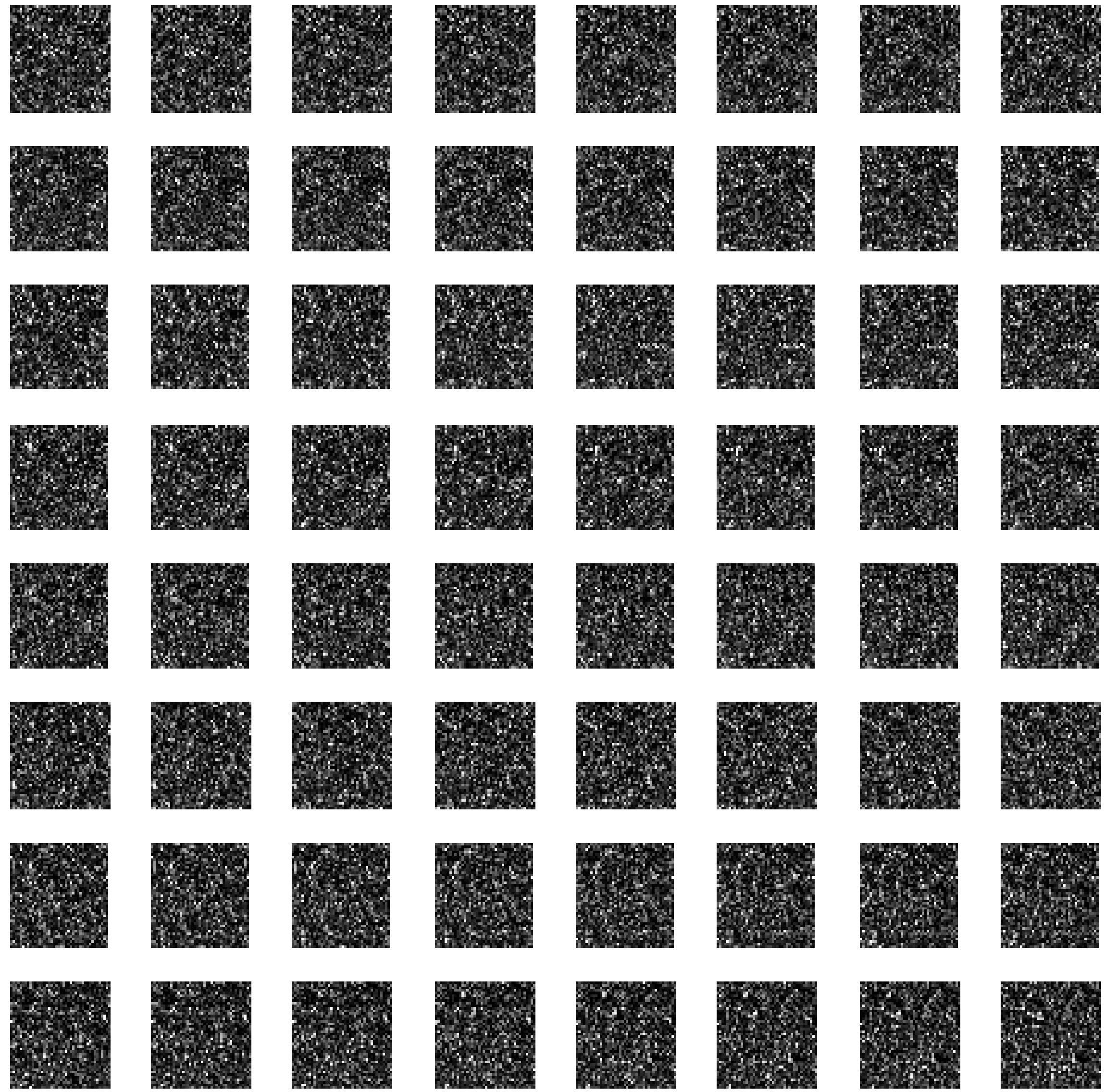

Imaging Correlography

- Get incoherent-image information from coherent speckle pattern
- Estimate 3-D Incoherent-object Fourier squared magnitude
  - Like Hanbury-Brown Twiss intensity interferometry

$$|F_{\mathrm{I}}(u,v,w)|^2 \approx \left\langle [D_k(u,v,w) - \mathrm{I}_o] \otimes [D_k(u,v,w) - \mathrm{I}_o] \right\rangle_k$$

(autocovariance of speckle pattern)

- Easier phase retrieval: have nonnegativity constraint on incoherent image
- Coarser resolution since correlography SNR lower

References:

P.S. Idell, J.R. Fienup and R.S. Goodman, "Image Synthesis from Nonimaged Laser Speckle Patterns," Opt. Lett. 12, 858-860 (1987).

J.R. Fienup and P.S. Idell, "Imaging Correlography with Sparse Arrays of Detectors," Opt. Engr. 27, 778-784 (1988).

J.R. Fienup, R.G. Paxman, M.F. Reiley, and B.J. Thelen, “3-D Imaging Correlography and Coherent Image Reconstruction,” in Proc. SPIE 3815-07, Digital Image Recovery and Synthesis IV, July 1999, Denver, CO., pp. 60-69.

The Institute of OPTICS

Image Autocorrelation from Correlography

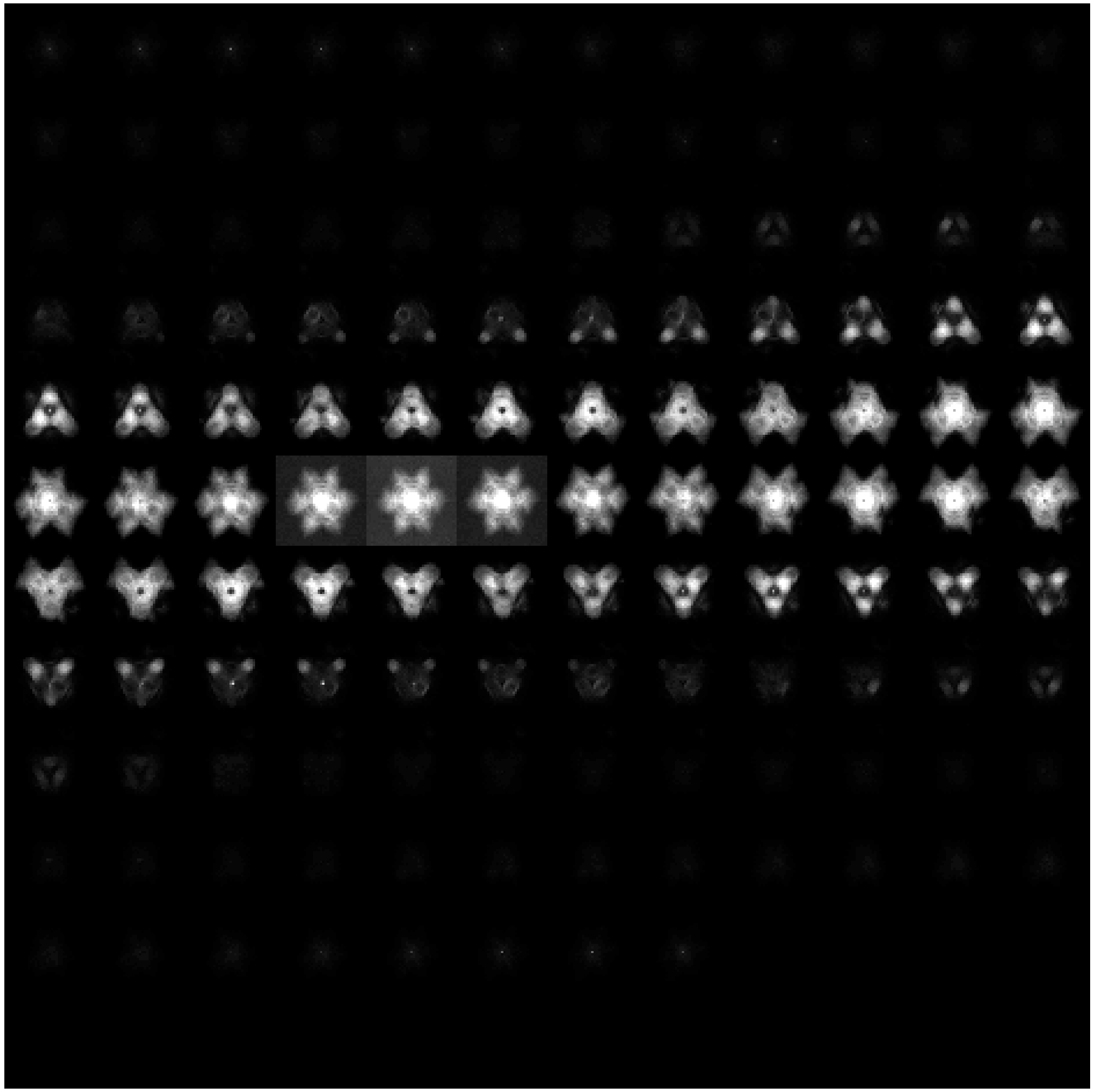

Thresholded Autocorrelation

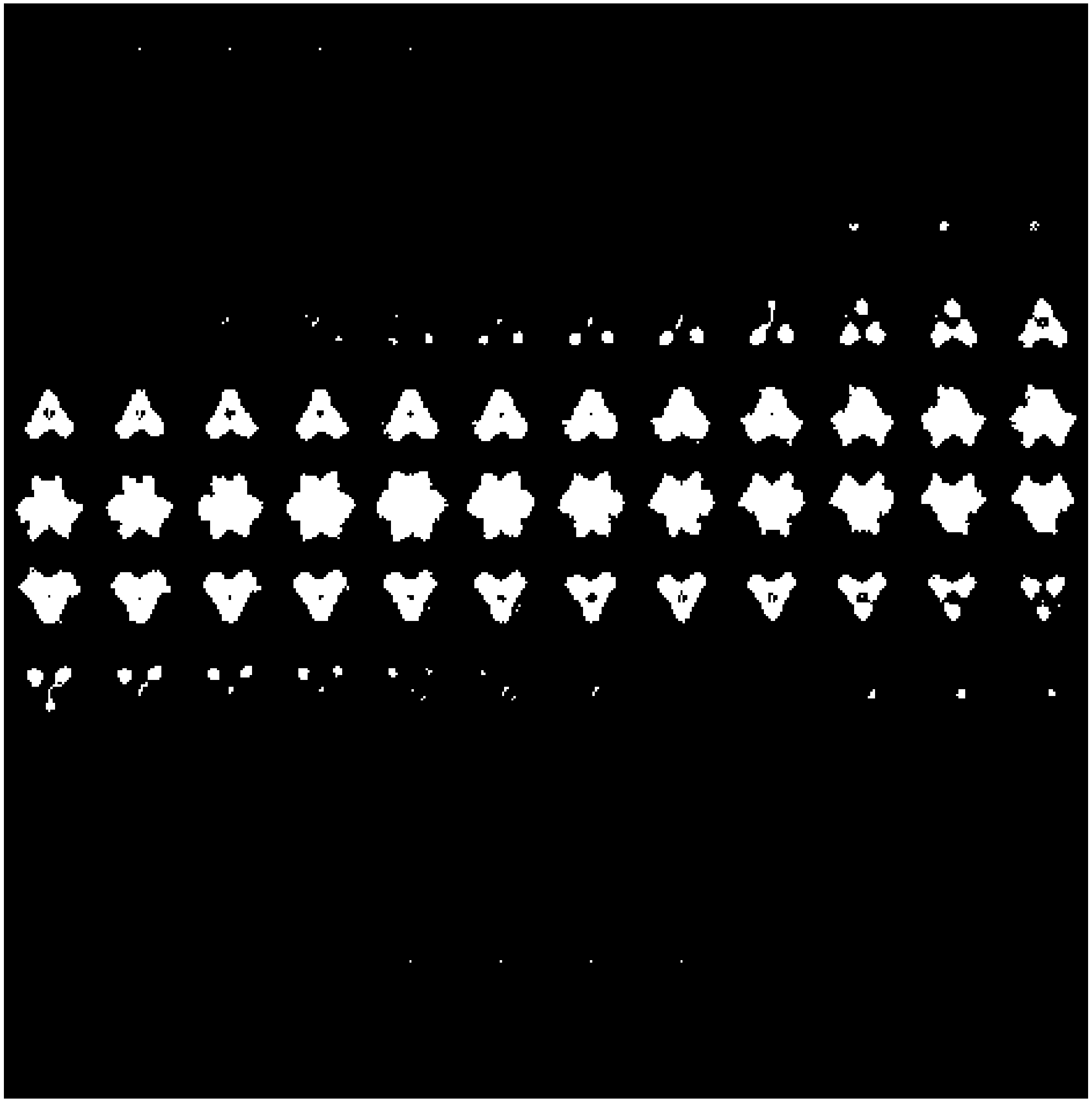

Triple Intersection of Autocorrelation Support

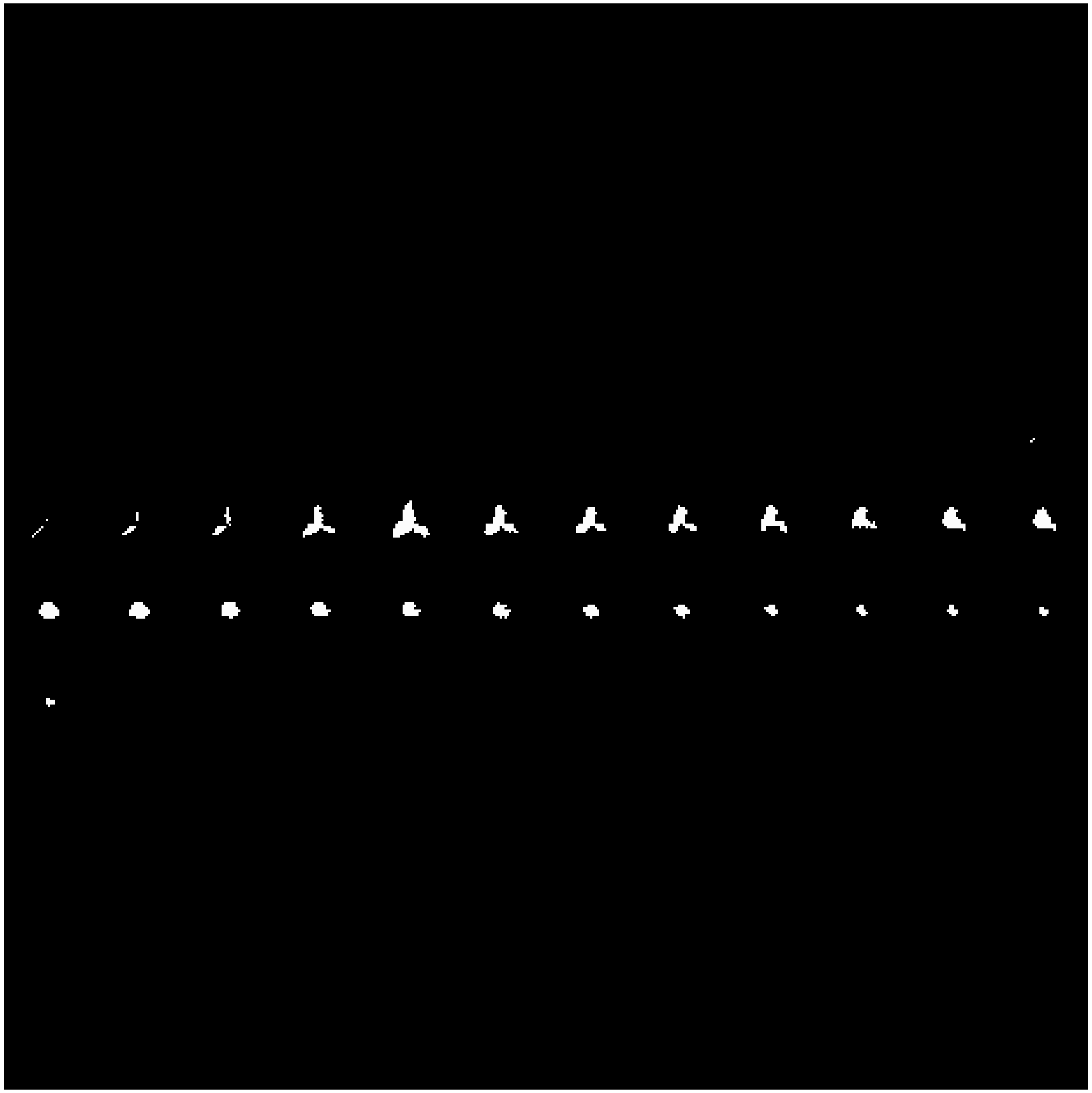

Locator Set, Slices 50-90

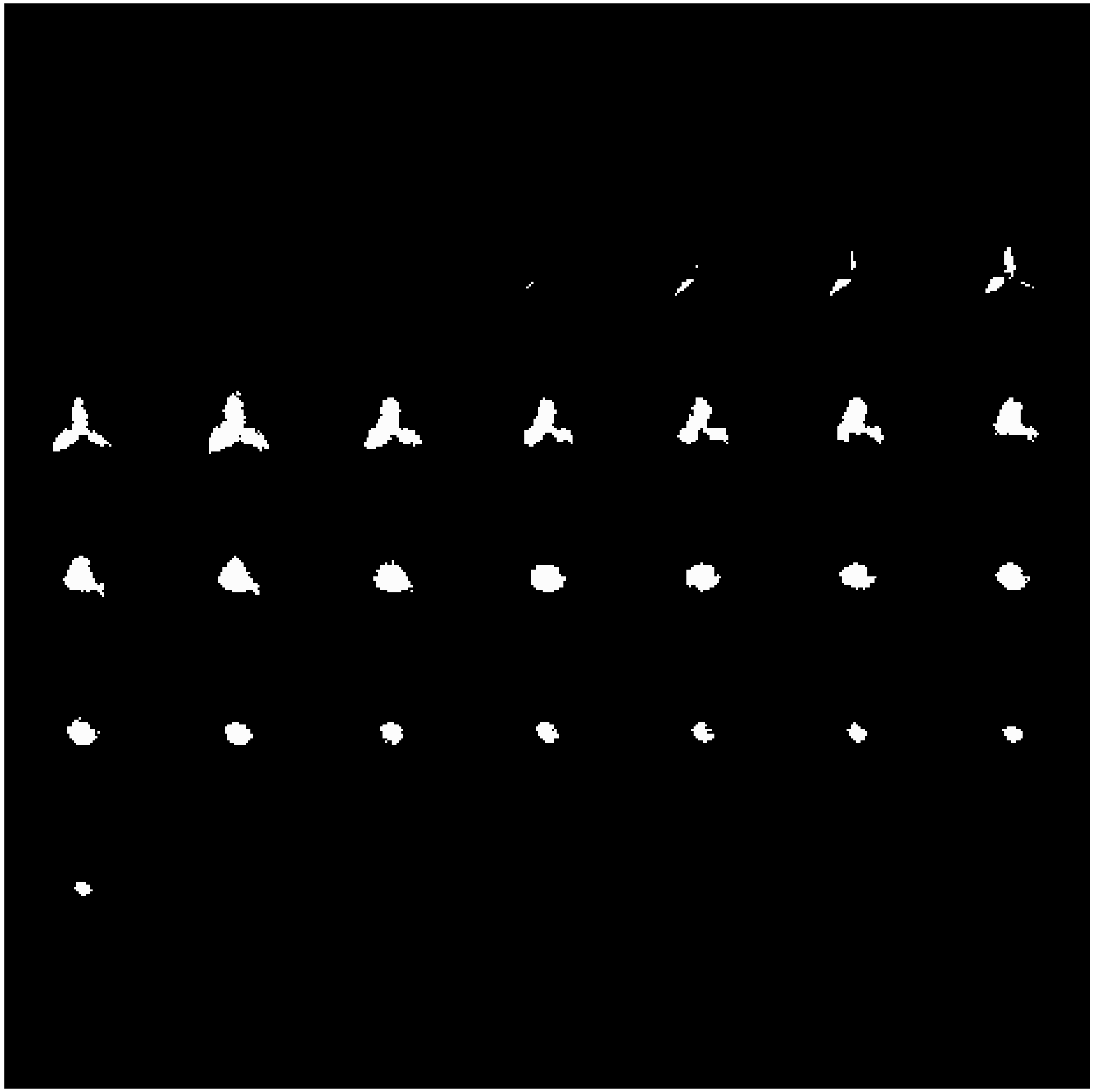

Dilated Locator Set used as Support Constraint

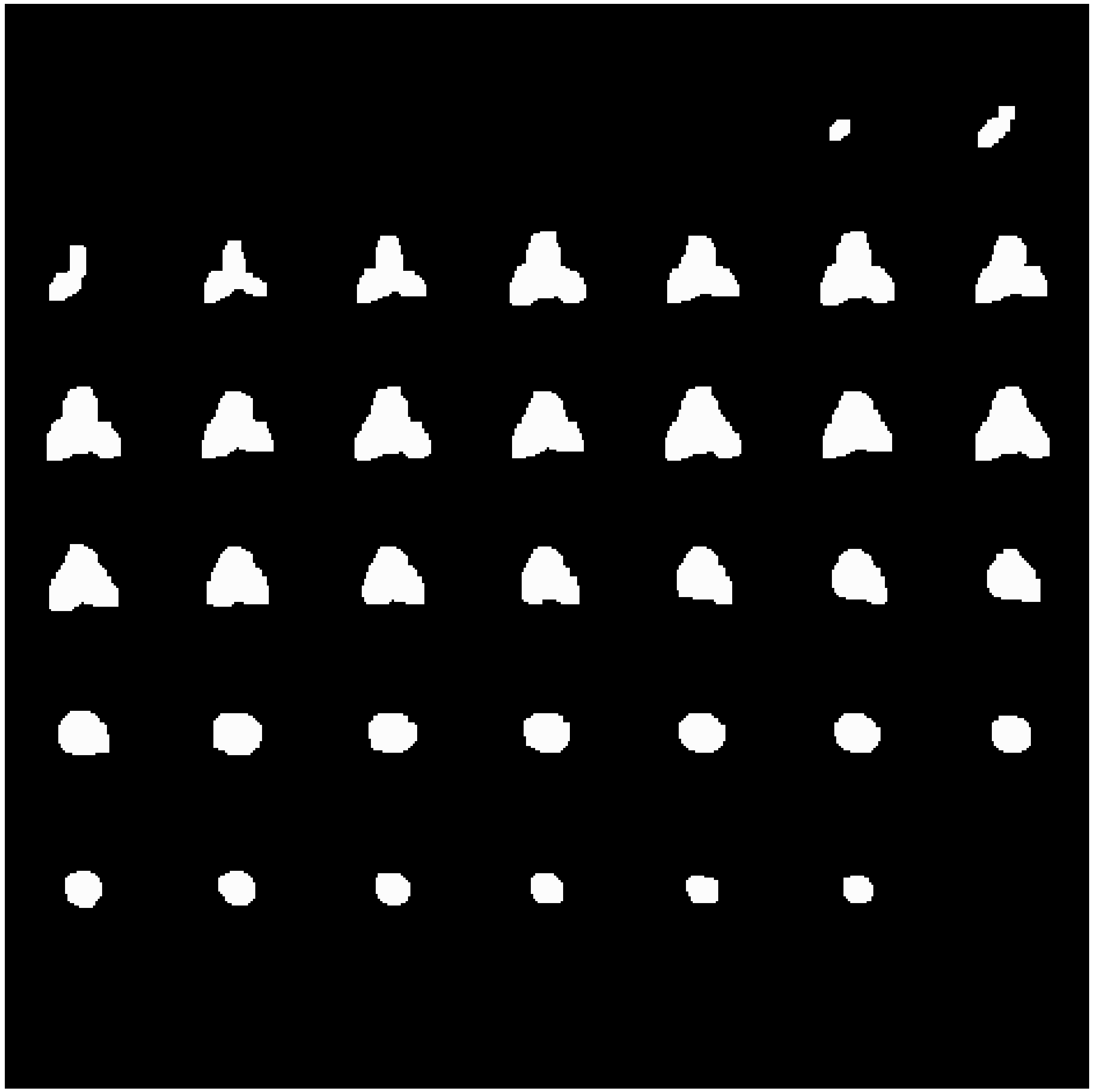

Fourier Modulus Estimate from Correlography

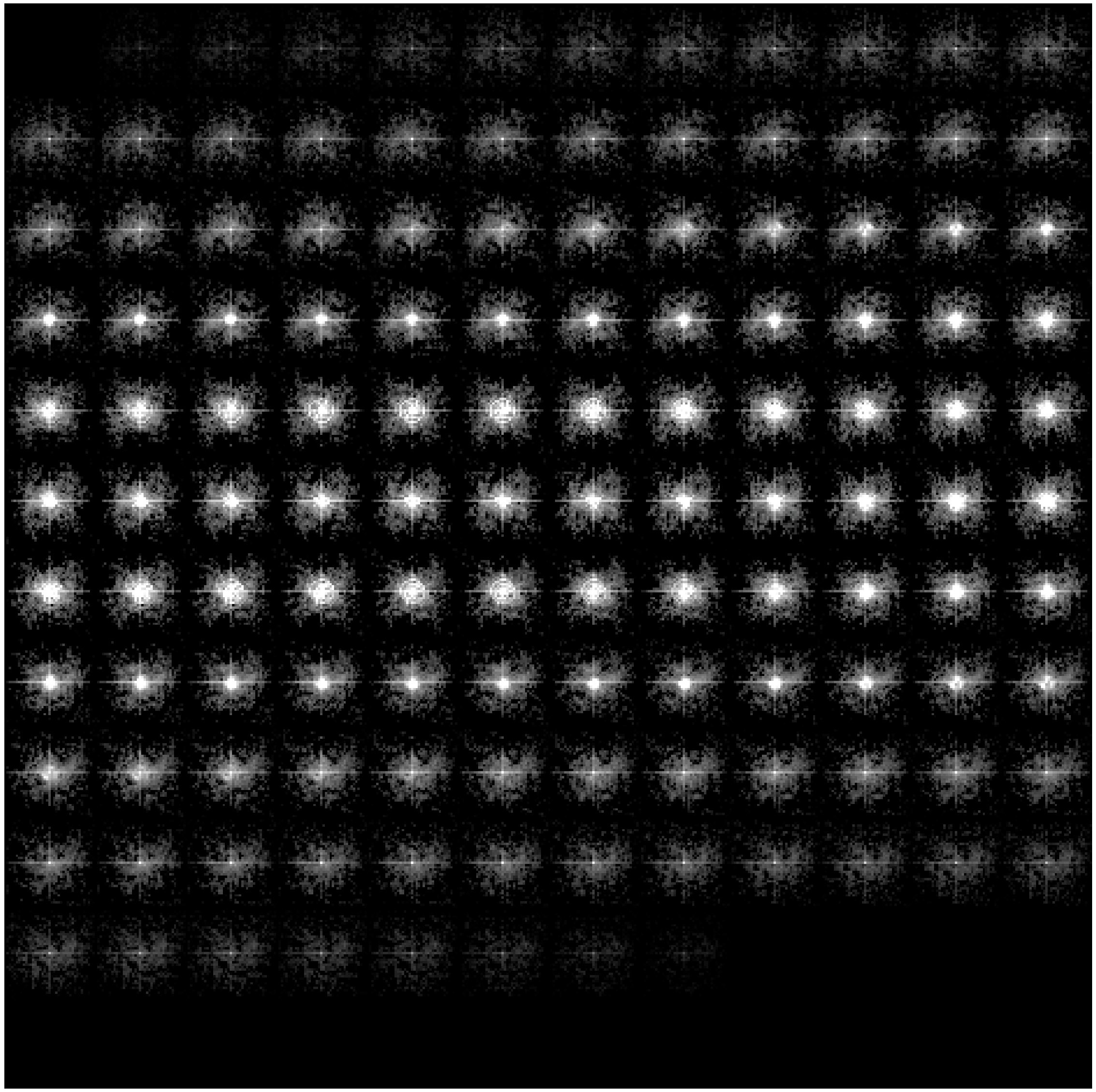

Fourier Magnitude, DC Slice

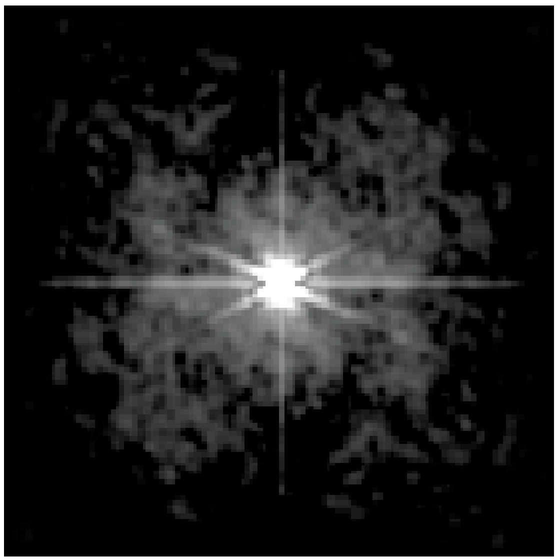

Before Filtering

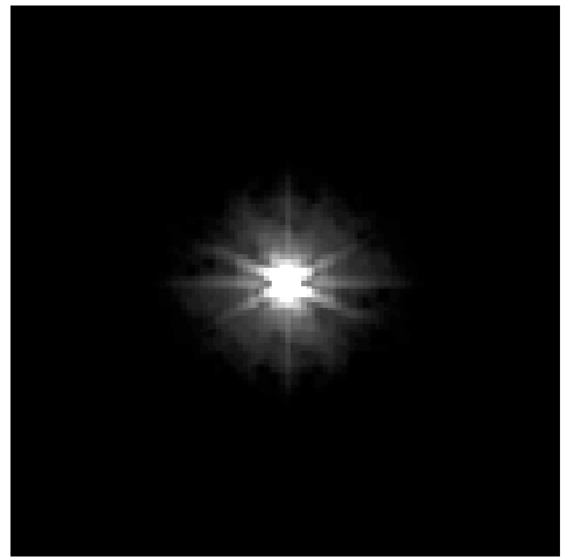

After Filtering

Incoherent Image Reconstructed by ITA

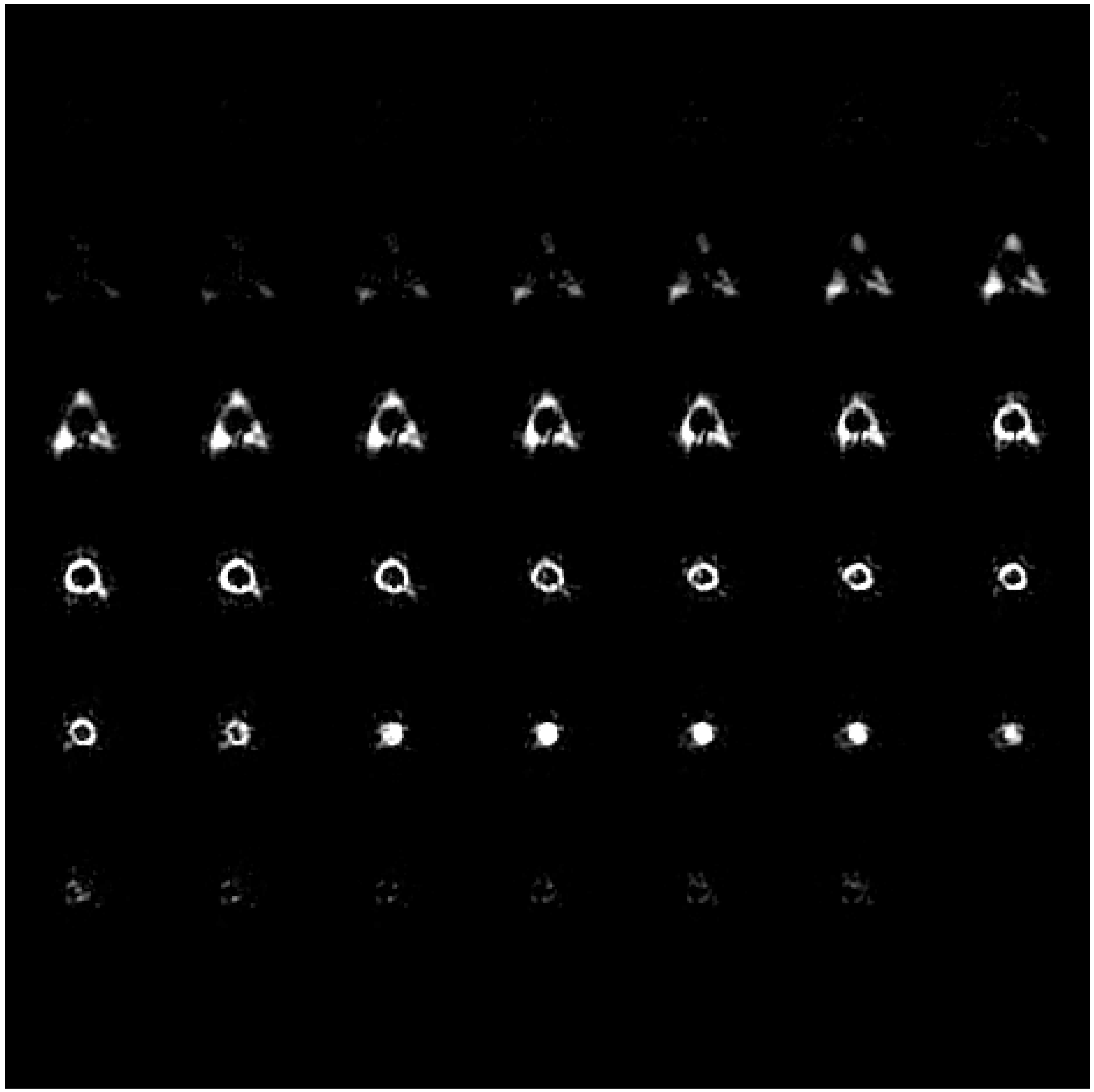

Support Constraint from Thresholded Incoherent Image

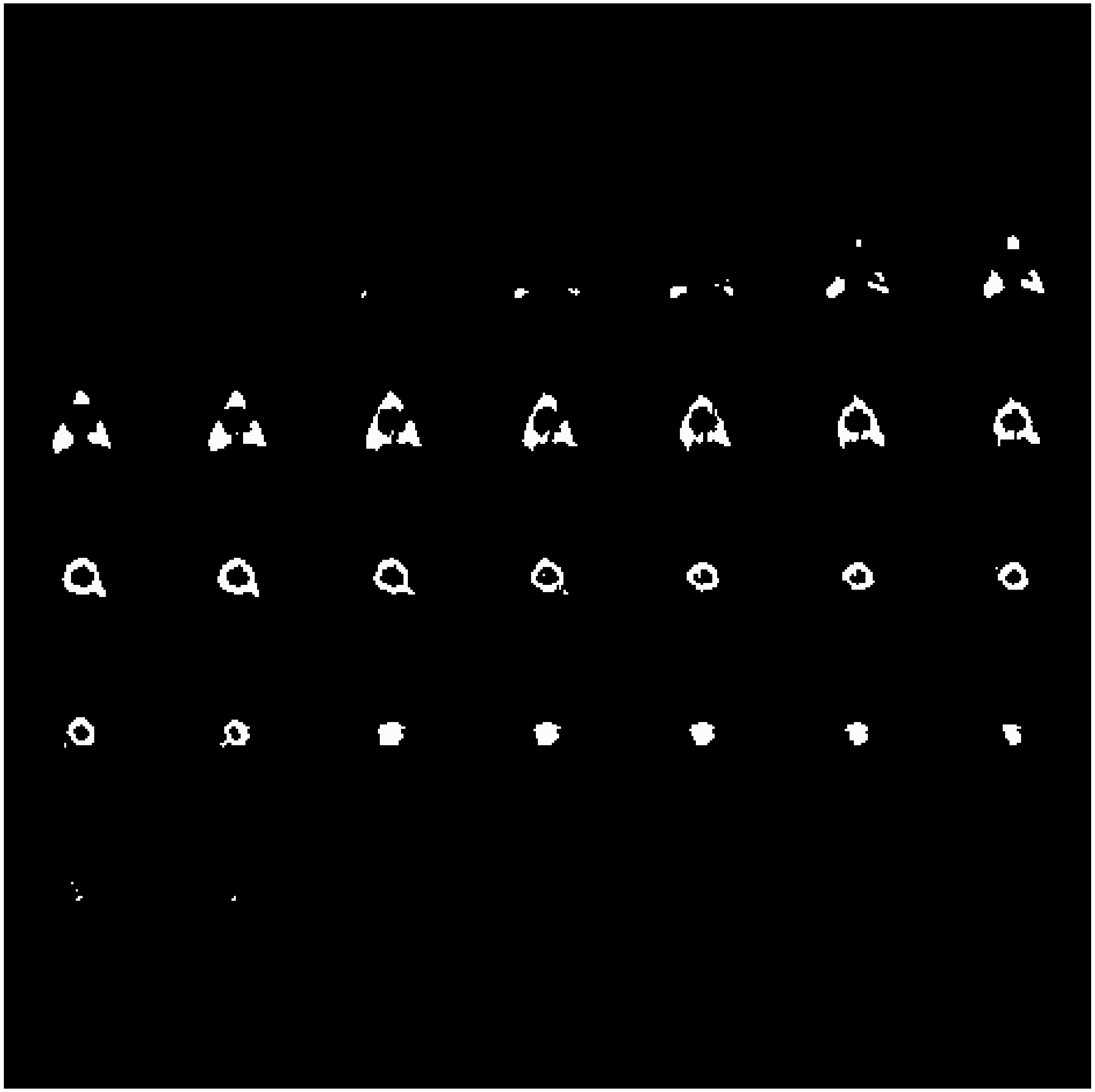

Dilated Support Constraint from Thresholded Incoherent Image

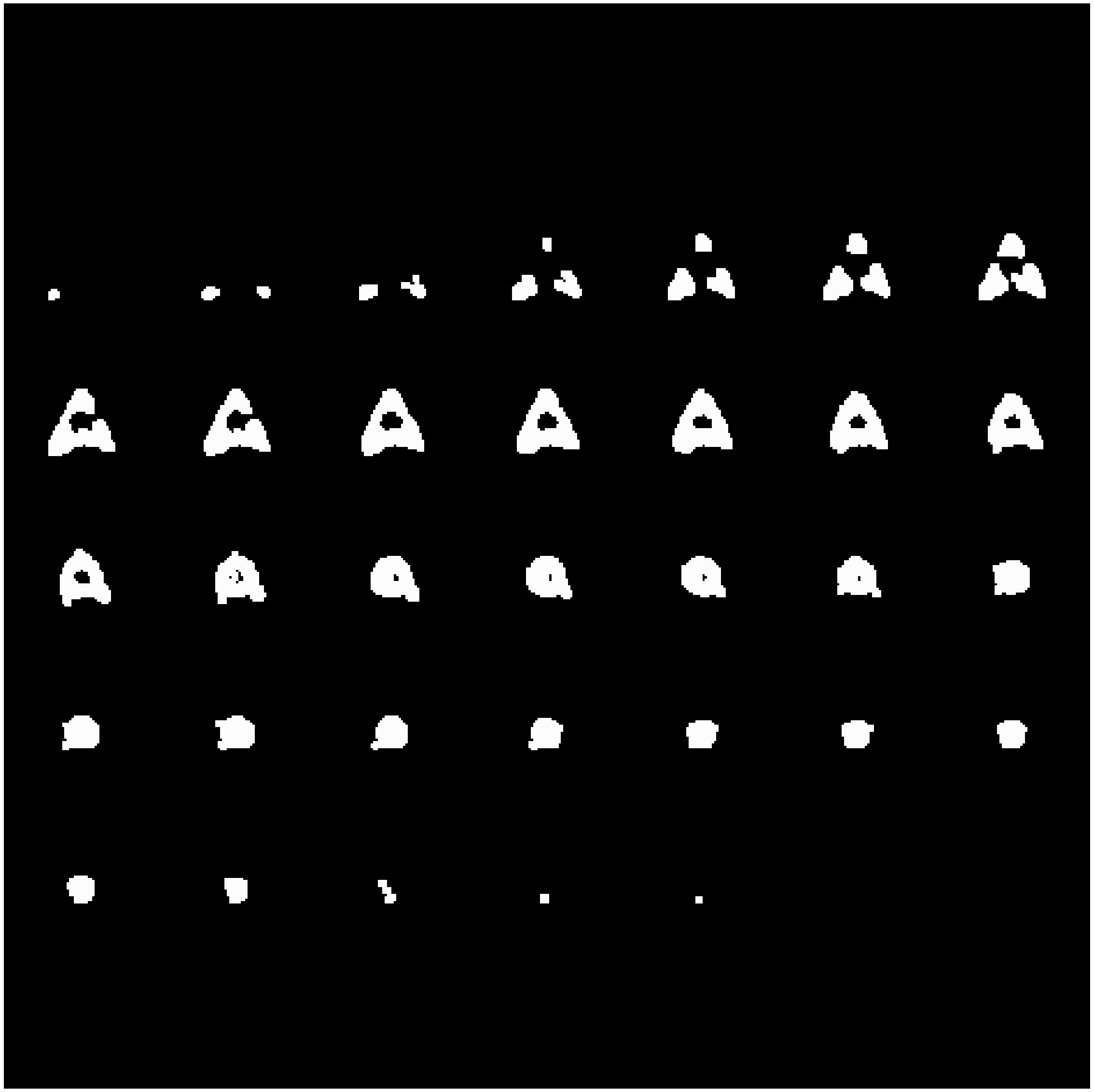

Coherent Image Reconstructed by ITA from One 128x128x64 Sub-Cube

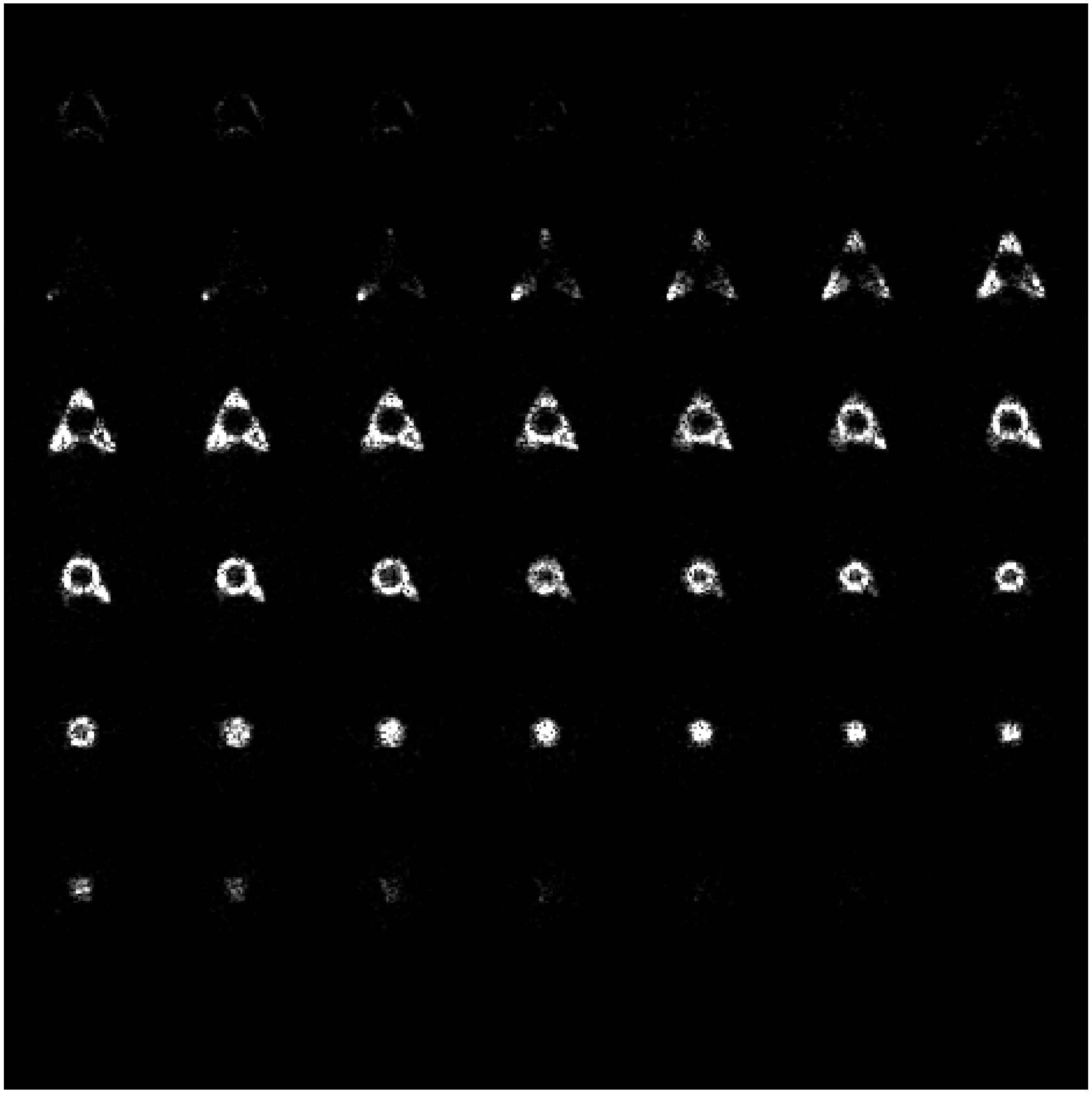

Example on Real X-Ray Data

(Data from M. Howells/LBNL and H. Chapman/LLNL)

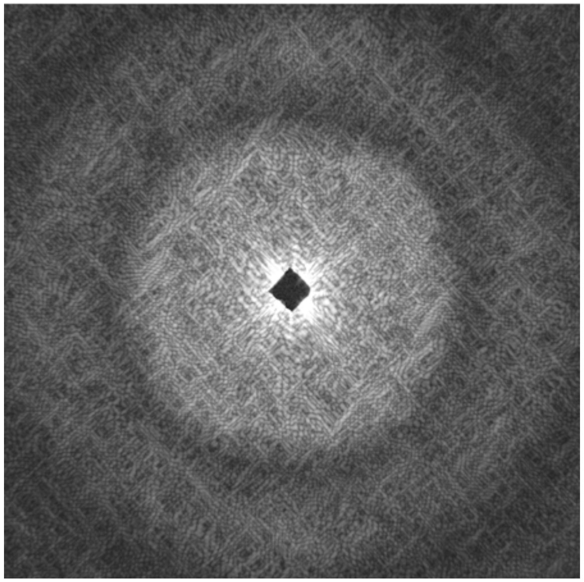

(a) X-ray data

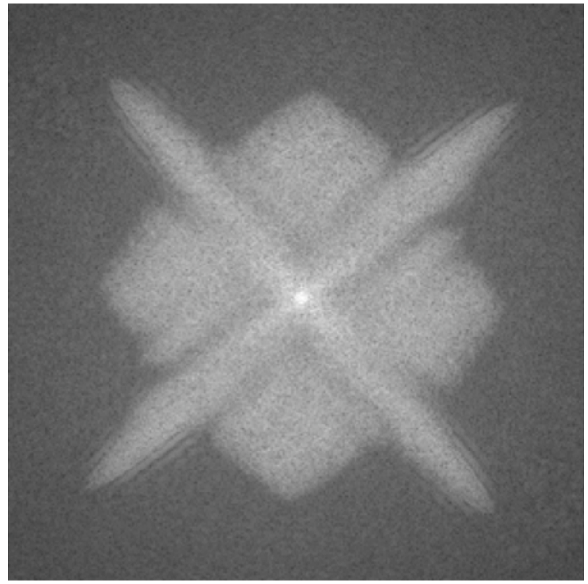

(b) Autocorrelation from (a)

(b) Triple Intersection

(c) Initial Support constraint computed from (b)

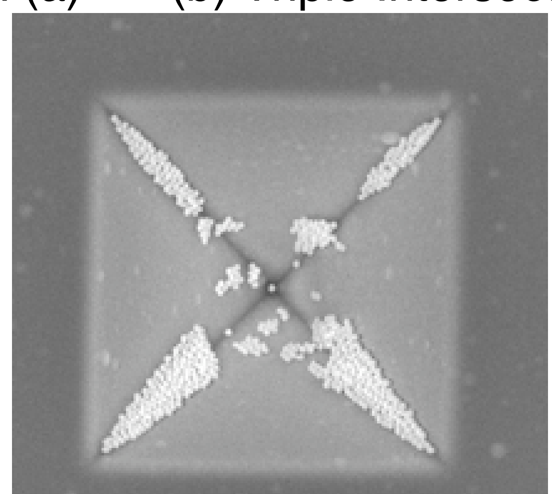

(d) Electron micrograph of object

Status of Support Estimation

- "Shrink wrap" algorithm tries to find support dynamically during iterations, but all other phase retrieval algorithms <u>need a support constraint</u>
- A low-resolution image of object by another sensor would help by providing a low-resolution support constraint, but phase retrieval works best with a fine-resolution support constraint
- Have several methods for fine-resolution support from autocorrelation
- Need to make support estimation from the autocorrelation more robust because of additional difficulties
  - Missing data at low spatial frequencies because of the beam stop
  - Complex-valued objects
  - High levels of noise in single frames
  - 3-D support estimation has been done [1], but not as mature as 2-D

[1] "3-D Imaging Correlography and Coherent Image Reconstruction," J.R. Fienup, R.G. Paxman, M.F. Reiley, and B.J. Thelen, in Proc. SPIE <u>3815</u>-07, <u>Digital Image Recovery and Synthesis IV</u>, July 1999, Denver, CO., pp. 60-69.

The Institute of OPTICS

References – 1

PROCLAIM:

R.G. Paxman, J.H. Seldin, J.R. Fienup, and J.C. Marron, "Use of an Opacity Constraint in Three-Dimensional Imaging," Proc. SPIE 2241-14, Inverse Optics III (April 1994), pp. 116-126.

R.G. Paxman, J.R. Fienup, J.H. Seldin and J.C. Marron, "Phase Retrieval with an Opacity Constraint," in Signal Recovery and Synthesis V, Vol. 11, 1995 OSA Technical Digest Series (Optical Society of America, Washington, DC, 1995), pp. 109-111.

M.F. Reiley, R.G. Paxman J.R. Fienup, K.W. Gleichman, and J.C. Marron, "3-D Reconstruction of Opaque Objects from Fourier Intensity Data," Proc. SPIE 3170-09, Image Reconstruction and Restoration 2, July 1997, pp. 76-87.

Support Reconstruction and Locator Sets:

J.R. Fienup, T.R. Crimmins, and W. Holsztynski, "Reconstruction of the Support of an Object from the Support of Its Autocorrelation," J. Opt. Soc. Am. 72, 610-624 (May 1982).

T.R. Crimmins, J.R. Fienup and B.J. Thelen, "Improved Bounds on Object Support from Autocorrelation Support and Application to Phase Retrieval," J. Opt. Soc. Am. A 7, 3-13 (January 1990).

J.R. Fienup, B.J. Thelen, M.F. Reiley, and R.G. Paxman, "3-D Locator Sets of Opaque Objects for Phase Retrieval," in Proc. SPIE 3170-10 Image Reconstruction and Restoration II, July, 1997, pp. 88-96.

References – 2

Imaging Correlography:

P.S. Idell, J.R. Fienup and R.S. Goodman, "Image Synthesis from Nonimaged Laser Speckle Patterns," Opt. Lett. 12, 858-860 (1987).

J.R. Fienup and P.S. Idell, "Imaging Correlography with Sparse Arrays of Detectors," Opt. Engr. 27, 778-784 (1988).

J.R. Fienup, R.G. Paxman, M.F. Reiley, and B.J. Thelen, “3-D Imaging Correlography and Coherent Image Reconstruction,” in Proc. SPIE 3815-07, Digital Image Recovery and Synthesis IV, July 1999, Denver, CO., pp. 60-69.

Iterative Transform Algorithm Phase Retrieval:

J.R. Fienup, “Phase Retrieval Algorithms: A Comparison,” Appl. Opt. 2l, 2758-2769 (1982).

J.R. Fienup, “Reconstruction of a Complex-Valued Object from the Modulus of Its Fourier Transform Using a Support Constraint,” J. Opt. Soc. Am. A 4, 118-123 (1987).

J.R. Fienup and A.M. Kowalczyk, “Phase Retrieval for a Complex-Valued Object by Using a Low-Resolution Image,” J. Opt. Soc. Am. A 7, 450-458 (1990).

Sidelobe Removal:

H.C. Stankwitz, R.J. Dallaire, and J.R. Fienup, “Non-linear Apodization for Sidelobe Control in SAR Imagery,” IEEE Trans. AES 31, 267-278 (1995).